Recent Advances in Calcium-Based Anticancer Nanomaterials Exploiting Calcium Overload to Trigger Cell Apoptosis

Yupeng Xiao, Zhao Li, Alberto Bianco, Baojin Ma

Recent Advances in Calcium-based Anticancer Nanomaterials Exploiting Calcium Overload to Trigger Cell Apoptosis

Yupeng Xiao[#], Zhao Li[#], Alberto Bianco, Baojin Ma**

Y. Xiao, Z. Li, B. Ma
Department of Tissue Engineering and Regeneration, School and Hospital of Stomatology, Cheeloo College of Medicine, Shandong University & Shandong Key Laboratory of Oral Tissue Regeneration & Shandong Engineering Laboratory for Dental Materials and Oral Tissue Regeneration
No. 44-1 Wenhuaxi Road, Jinan, Shandong, 250012, China
E-mail: baojinma@sdu.edu.cn (B. Ma)

A. Bianco
CNRS, Immunology, Immunopathology and Therapeutic Chemistry, UPR3572, University of Strasbourg, ISIS
No. 2, allée Konrad Roentgen, Strasbourg, 67000, France
E-mail: a.bianco@ibmc-cnrs.unistra.fr (A. Bianco)

[#] These authors contributed equally.

Keywords: calcium phosphate nanoparticles, cell uptake, oxidative stress, endoplasmic reticulum, Ca^{2+} channels

Abstract

Calcium ion is vital for the regulation of many cellular functions and serves as a second messenger in the signal transduction pathways. Once the intracellular Ca^{2+} level exceeds the tolerance of cells (called Ca^{2+} overload), oxidative stress, mitochondrial damage and cell/mitochondria apoptosis happen. Therefore, Ca^{2+} overload has started to be deeply exploited as a new strategy for cancer therapy due to its high efficiency and satisfactory safety. This review aims to highlight the recent development of Ca^{2+}-based nanomaterials (such as $Ca_3(PO_4)_2$, $CaCO_3$, CaO_2, CaH_2, CaS, and others) able to trigger intracellular Ca^{2+} overload and apoptosis in cancer therapy. The intracellular mechanisms of varied Ca^{2+}-based nanomaterials and the different types of strategies to enhance Ca^{2+} overload are discussed in detail. Moreover, the design of more efficient Ca^{2+} overload-mediated cancer therapies is prospected mainly based on (1) the enhanced cellular uptake by surface modification and morphology optimization of nanomaterials, (2) the accelerated Ca^{2+} release from nanomaterials by increasing the intracellular H^+ level and by photothermal effect, and (3) the overload maintenance by Ca^{2+} efflux inhibition, Ca^{2+} influx promotion, or promoting Ca^{2+} release from the endoplasmic reticulum.

1. Introduction

Intracellular Ca^{2+} plays a pivotal role in many physiological processes, including proliferation, differentiation, apoptosis, the transmission of neural excitation, and contraction of the muscles.[1] In non-muscle cells (e.g., endothelial cells, fibroblasts, pericytes, and macrophages), Ca^{2+} is mainly stored in the endoplasmic reticulum (ER).[2-4] Owing to the efficient storage, intracellular Ca^{2+} can serve as a second messenger in the signal transduction pathways including IP_3 (inositol triphosphate)-triggered Ca^{2+} release for regulation of the activity of numerous downstream targets (e.g., protein kinase C).[5-7] Ca^{2+} signaling generated by ER can be regulated by the mitochondria, and the cytoplasmic Ca^{2+} released from ER can be rapidly restored into ER with the assistance of mitochondria.[8-10] These processes constitute the intracellular Ca^{2+} signal networks.[11-13] Meanwhile, the contraction and relaxation behaviors of the muscles are controlled by Ca^{2+} through three major mechanisms, including the troponin-tropomyosin system, the calmodulin (CaM) system, and the direct binding of Ca^{2+} to myosin.[1,14,15] Ca^{2+} is also indispensable in the generation of electrical signals and signal transmission between neurons on nerve fibers.[16,17] Therefore, Ca^{2+} is vital for the regulation of cellular behavior and fate.

However, the dysfunction of calcium homeostasis would cause severe cell stress and sometimes cell death. Indeed, treating cells with apoptotic stimuli, like C_2-ceramide, can induce Ca^{2+} release from ER, increasing the cytoplasmic Ca^{2+} level and changing the morphological characteristics of mitochondria.[18-20] Once the intracellular Ca^{2+} level exceeds the tolerance of cells (identified as Ca^{2+} overload), particularly combined with pathological conditions of oxidative stress, cell apoptosis is occurring.[21,22] For example, it has been demonstrated that the increase of intracellular Ca^{2+} is required for the activation of mitochondrial calpain to release apoptosis-inducing factor (AIF) to trigger cell death.[23-25] AIF can translocate into the nucleus, and participate in chromatin condensation and large-scale DNA fragmentation, causing cell apoptosis. The sustained Ca^{2+} overload also could cause the opening of cyclophilin D-dependent mitochondrial membrane pores and the loss of oxidative phosphorylation due to the formation of calcium phosphate precipitation, inducing energy exhaustion.[26,27]

With the development of nanotechnology, cell apoptosis caused by Ca^{2+} overload can be regulated by functional nanomaterials, developed as a new cancer strategy (called Ca^{2+} interference therapy).[28] Ca^{2+}-based nanomaterials (such as $Ca_{10}(PO_4)_6(OH)_2$, $CaCO_3$, and CaO_2) as Ca^{2+} overload regulators have an acid-response property, meaning that they can release abundant Ca^{2+} by responding to the tumor microenvironment (TME), thus increasing the intracellular Ca^{2+} level and inducing cell apoptosis and death. Due to these characteristics,

Ca^{2+}-based nanomaterials have been recently widely applied in cancer therapy by triggering intracellular Ca^{2+} overload. Moreover, Ca^{2+}-based nanomaterials are usually low cost, due to the simple preparation methods and cheap raw materials, and possess relatively high biosecurity owing to the biocompatible components. Furthermore, Ca^{2+} overload-mediated cancer therapy does not need to require external stimulations like photothermal therapy (PTT), photodynamic therapy (PDT), and sonodynamic therapy (SDT), which is beneficial for wide biomedical applications and clinical translation. Therefore, Ca^{2+} overload-mediated cancer therapy has attracted more and more attention. Although two reviews of calcium-based biomaterials for diagnosis and therapy have very recently appeared, they mainly reported on various therapeutic strategies and calcification-mediated computed tomography imaging, rather than focusing on and discussing the opportunity of Ca^{2+} overload-mediated cancer therapy.[29,30]

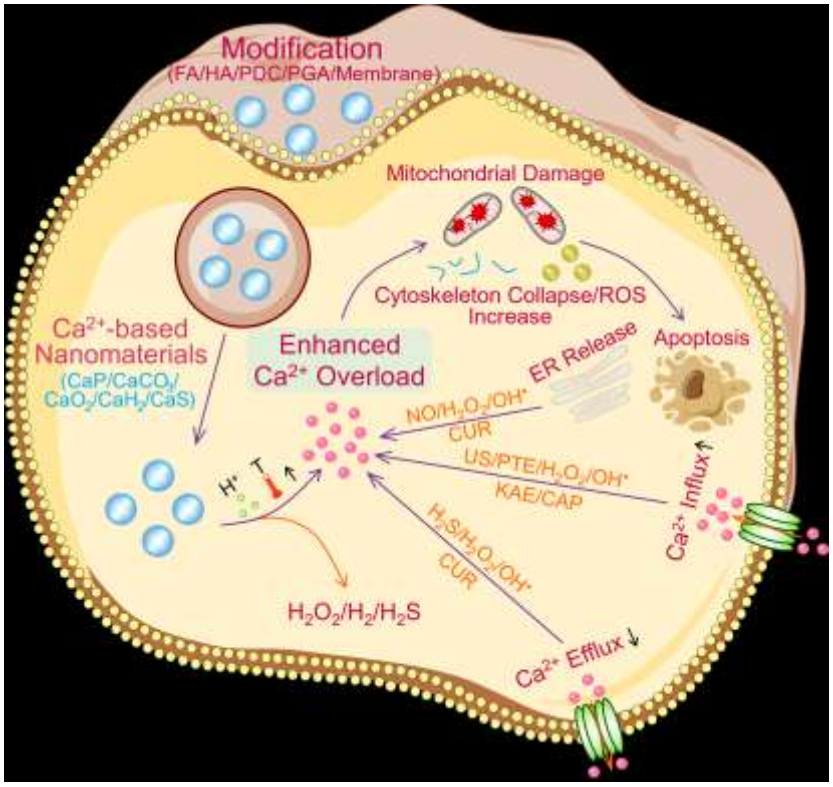

Figure 1. Schematic illustration of enhanced Ca^{2+} overload.

In this review, different types of Ca^{2+}-based nanomaterials will be discussed in detail, especially focusing on the action mechanisms and synergistic effects (e.g., enhanced endocytosis, Ca^{2+} efflux inhibition, Ca^{2+} influx promotion, triggering Ca^{2+} release from ER, accelerated Ca^{2+} release from nanomaterials and so on) to further enhance intracellular Ca^{2+} level and amplify Ca^{2+} overload (**Figure 1**). We would like to underline that our review is also alternative and different from a very recent review that mainly focuses on the combination of Ca^{2+} overload with other cancer therapeutic strategies rather than enlighting the potential to

enhance the self-efficiency of Ca^{2+} overload-mediated cancer therapy.[31] Therefore, our review provides a targeted discussion about this new cancer therapy modality, which could inspire new ideas in designing increased efficiency systems and broadening its biomedical applications.

2. Ca^{2+}-based Anticancer Nanomaterials

This section is divided into four parts based on the types of Ca^{2+}-based nanomaterials, describing conventional $Ca_3(PO_4)_2$, $CaCO_3$, CaO_2, and other new nanomaterials, respectively. The intracellular mechanisms of action and the unique advantages of each nanosystem are described.

2.1 Calcium Phosphate-based Nanomaterials

Calcium phosphate (CaP)-based nanomaterials widely exist in biological hard tissues such as teeth and bones. The common CaP-based nanomaterials include hydroxyapatite (Hap, $Ca_{10}(PO_4)_6(OH)_2$), tricalcium phosphate (TCP, $Ca_3(PO_4)_2$), or monocalcium phosphate monohydrate ($Ca(H_2PO_4)_2{\cdot}H_2O$).[32] Synthetic CaP-based nanomaterials are similar to the natural form and possess high biocompatibility and good biodegradability.[33] Besides, some innate properties of CaP-based nanomaterials such as pH-sensitive solubility and easy methods of preparation make them useful in targeted tumor therapy.[34]

As the main inorganic component of bone, HAp has been widely used in the biomedical field.[35-37] Rod-like HAp nanoparticles (HAp NPs) were synthesized by coprecipitation and calcination and showed excellent selective anticancer activity (**Figure 2**a).[38] Cancer cells can internalize more HAp NPs than normal cells, leading to a sustained high Ca^{2+} concentration (Figure 2b and c). The different intracellular Ca^{2+} concentrations showed different effects on the diverse types of cells. HAp NPs had little effect on normal cells. Inversely, HAp NPs can cause cancer cell death by inducing mitochondrial damage and apoptosis. Besides, the distribution of HAp NPs in normal cells and cancer cells was investigated using fluorescent probes. In cancer cells, the HAp NPs signals were largely colocalized with the mitochondria, indicating that HAp NPs had the targeting ability to induce mitochondrial Ca^{2+} overload. The mitochondrial targeting of HAp NPs might be mainly triggered by cell-type specific mechanisms, due to the altered metabolic pattern in cancer cells. However, the detailed mechanism for this targeting ability still needs to be further studied. To complement the *in vitro* data, the *in vivo* antitumor efficacy and safety of HAp NPs were investigated. The growth rate of xenografted human lung tumors (using A549 cells) decreased after HAp NPs treatment (Figure 2d). Meanwhile, no obvious body weight changes and organ damage were observed

after being treated with HAp NPs three times a week for 26 days. Furthermore, to amplify the Ca^{2+} overload, ultrathin HAp nanosheets doped with pyrazine-2,3-dicarbonitrile (HAp-PDCns) were prepared to enhance the internalization of HAp into cancer cells via clathrin-mediated endocytosis, and selectively concentrate it in the charged mitochondrial membrane.[39] The proton-triggered decomposition of HAp-PDCns causes mtDNA damage by an instantaneous local Ca^{2+} overload in the mitochondria of cancer cells, leading to an inhibition of tumor growth. To endow HAp with targeting ability, polyacrylic acid (PAA)-coordinated HAp NPs chemically grafted with folic acid (HAp-PAA-FA) were prepared.[40] These spherical HAp-PAA NPs exhibited good tumor cell death. After linking FA, HAp-PAA-FA NPs can target cancer cells better, specifically killing these cells.

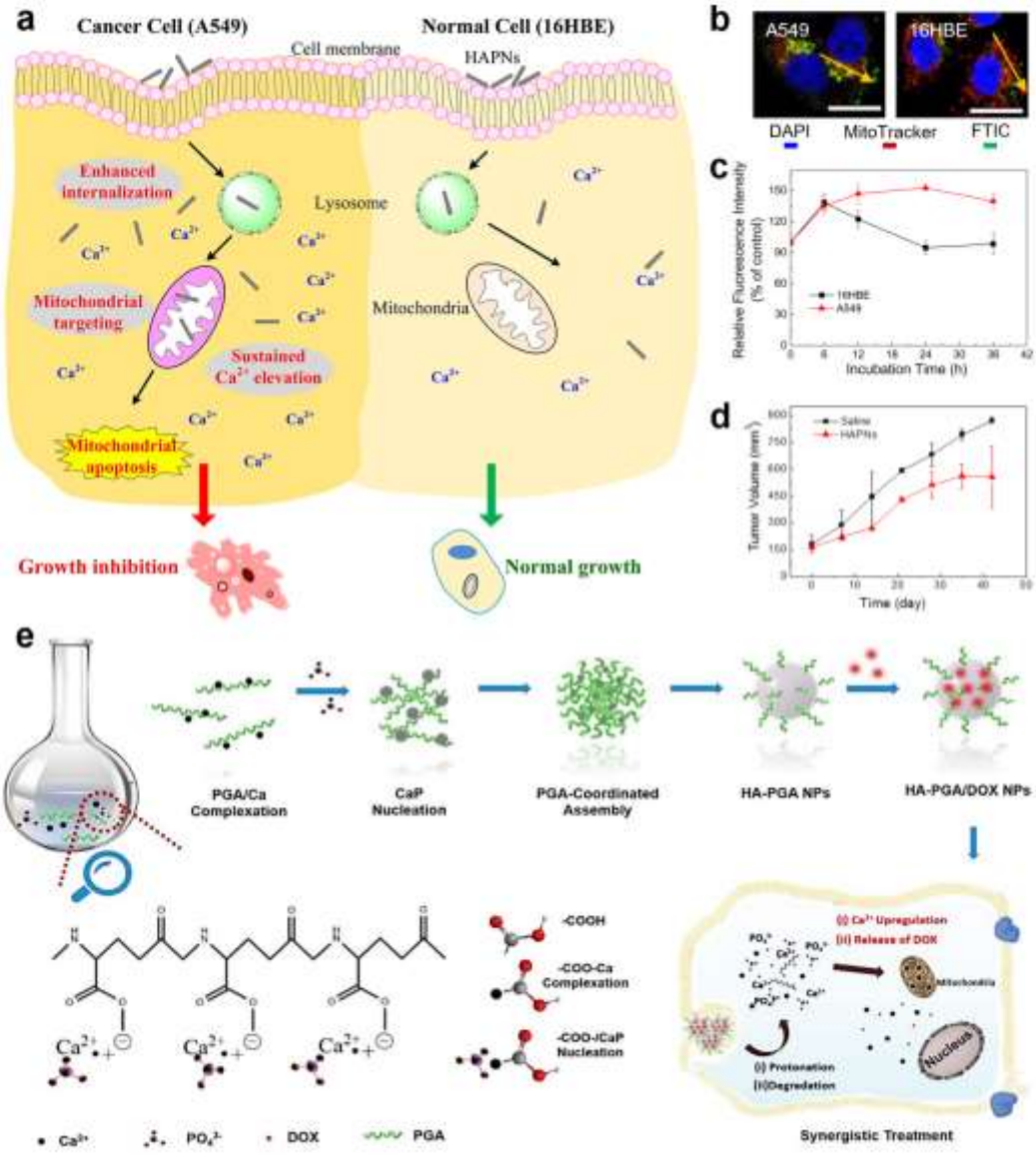

Figure 2. a) Schematic illustration of HAp NPs-mediated apoptosis and tumor growth inhibition; b) Selective accumulation of fluorescently labeled HAp NPs in cancer cells' mitochondria after 48 h incubation. The green and red fluorescence represent FITC-HAp NPs

and MitoTracker, respectively; c) Relative fluorescence intensity change of intracellular Ca^{2+} in normal and cancer cells with time. Reproduced with permission.[38] Copyright 2016, American Chemical Society; d) Volume change of xenografted A549 cell tumor; e) Schematic illustration of HA-PGA/DOX-mediated synergistic treatment. Reproduced with permission.[41] Copyright 2019, Royal Society of Chemistry.

Unfortunately, HAp alone can only inhibit tumor growth to a certain degree. To obtain more efficient cancer treatment, the combination of HAp NPs with antitumor drugs is a promising strategy. For this purpose, a so-called "calcium ion nanogenerator" (TCaNG) was designed by combining HAp with doxorubicin (DOX).[42] TCaNG was able to induce Ca^{2+} bursting release in lysosomes and then reverse drug resistance by suppressing cellular respiration and blocking intracellular ATP production. Interestingly, TCaNG can decrease the IC50 of DOX to resistant MCF-7/ADR cells by ~30 times and reduce the proliferation of drug-resistant tumors by approximately 13 times without obvious side effects. To simultaneously achieve an enhanced Ca^{2+} overload and an efficient chemotherapeutic effect of DOX, a polyglutamic acid (PGA)-combined assembly of HAp NPs (HAp-PGA NPs) was designed (Figure 2e).[41] After being modified by PGA, more HAp NPs were internalized into cancer cells, bringing a highly sustained Ca^{2+} level. The dramatic elevation of intracellular Ca^{2+} induced a cascade of mitochondrial membrane damage and ATP content reduction, which activated apoptosis and upregulated the drug sensitivity to chemotherapy, respectively. Furthermore, it is known that DOX is released in a pH-responsive manner. With the synergistic effects of DOX and enhanced calcium overload, a selectively intensified toxicity to tumor cells was achieved. *In vivo* results further confirmed that the combined therapy mediated by HAp-PGA/DOX exhibited highly selective tumor inhibition and reduced heart toxicity.

Because the acid response of CaP is weak and the release of Ca^{2+} is not enough sufficient, the therapeutic efficacy is unsatisfactory due to a weak Ca^{2+} overload. To increase the level of intracellular Ca^{2+} and enhance Ca^{2+} overload, Xu et al. developed a doubly enhanced Ca^{2+} nanogenerator (DECaNG) based on TCP combined with curcumin (CUR) and photothermal effect (PTE) (**Figure 3**a).[43] CUR is a polyphenol extracted from the dietary spice turmeric and herb. As a bioactive agent, CUR can inhibit Ca^{2+} transfer from the cytoplasm to the extracellular compartment and promote Ca^{2+} release from the ER to the cytoplasm, thus increasing Ca^{2+} concentration in the mitochondria, resulting in a mitochondrial Ca^{2+} overload state.[44] The copper sulfide (CuS) was used to hybridize with TCP because of the hydrophilicity and the high drug loading capacity.[45] Besides, CuS NPs exert a PTE under near-infrared (NIR) light

radiation, which not only showed great promise for PTT of tumors,[46] but also promoted the release of Ca^{2+}.[47] Based on the innate advantages of TCP and these ways to enhance the therapeutic effects, DECaNG could effectively induce cancer cell apoptosis. In the acidic environment of lysosomes, Ca^{2+} was released efficiently, being DECaNG pH-sensitive. The PTE of CuS could further promote Ca^{2+} release by causing a structural instability of TCP.[48] Due to the acid response in lysosomes, a lot of Ca^{2+} was released from DECaNG especially under NIR light irradiation, causing the intracellular Ca^{2+} level to remarkably increase (Figure 3b and c). Moreover, the abundant Ca^{2+} produced by DECaNG was observed to flow into mitochondria, leading to a decreased mitochondrial membrane potential and triggering cell apoptosis (Figure 3d). To confirm the detailed mechanism of apoptosis, the expressions of caspase-3, cytochrome c, and Bcl-2 were measured by Western blot (Figure 3e). Caspase-3 was activated in all different treatment groups, but most in the DECaNG group. In parallel, the amount of cytochrome c increased, and antiapoptotic protein Bcl-2 decreased, indicating the initiation of the mitochondria-mediated apoptosis pathway. Due to the structural damage and dysfunction of mitochondria, the content of ATP decreased especially in the DECaNG group (Figure 3f). Importantly, *in vivo* results showed that DECaNG possessed an efficient antitumor effect (Figure 3g). Ca^{2+} content in the tumor tissues of the DECaNG group was dramatically higher than that in the saline group (Figure 3h), with many cancer cells undergoing apoptosis (Figure 3i). Therefore, DECaNG showed great potential for cancer treatment via the synergy of chemotherapy, thermotherapy, and enhanced mitochondrial Ca^{2+} overload.

In an alternative approach, amorphous CaP nanosystems were also designed to treat cancer.[49-51] CaP-black phosphorus nanosheets (CaBPs) were synthesized by *in situ* mineralization strategy.[50] Compared to BPs alone, CaBPs exhibited enhanced and selective anticancer bioactivity due to the improved pH-responsive degradation behavior and intracellular Ca^{2+} overload in cancer cells. Interestingly, CaBPs specifically targeted and damaged mitochondria, causing mitochondria-mediated apoptosis in cancer cells. *In vivo* results demonstrated that CaBPs can target orthotopic breast cancer cells to inhibit tumor growth without obvious adverse side effects. Furthermore, amorphous CaP loaded with DOX and modified by RGD showed good efficiency for tumor inhibition by ROS-enhanced Ca^{2+} overload and chemotherapy.[52]

It has been reported in several papers that autophagy degrades dysfunctional organelles to sustain metabolism and homeostasis, participating in resistance to PDT.[53-55] In this context, complementary mitochondrial Ca^{2+} overload and autophagy inhibition were used to cover the shortage of PDT. Wang et al. designed biodegradable tumor-targeted inorganic/organic hybrid

nanocomposites (DPGC/OI) synchronously encapsulating IR780 and obatoclax (an autophagy inhibitor) by biomineralization of the nanofilms, which consist of pH-triggered CaP and long circulation phospholipid block copolymers 1,2-distearoyl-sn-glycero-3-phosphoethanolamine (DSPE)-poly(ethylene glycol) (PEG)2000-glucose (DPG).[56] In the presence of the hydrophilic PEG chain and the glucose transporter 1 (Glut-1) ligand, sufficient enrichment of DPGC/OI in tumor tissues was achieved. The combination of Ca^{2+} overload, IR780 mediated PDT, and obatoclax-caused autophagy inhibition endowed DPGC/OI with a high therapeutic effect.

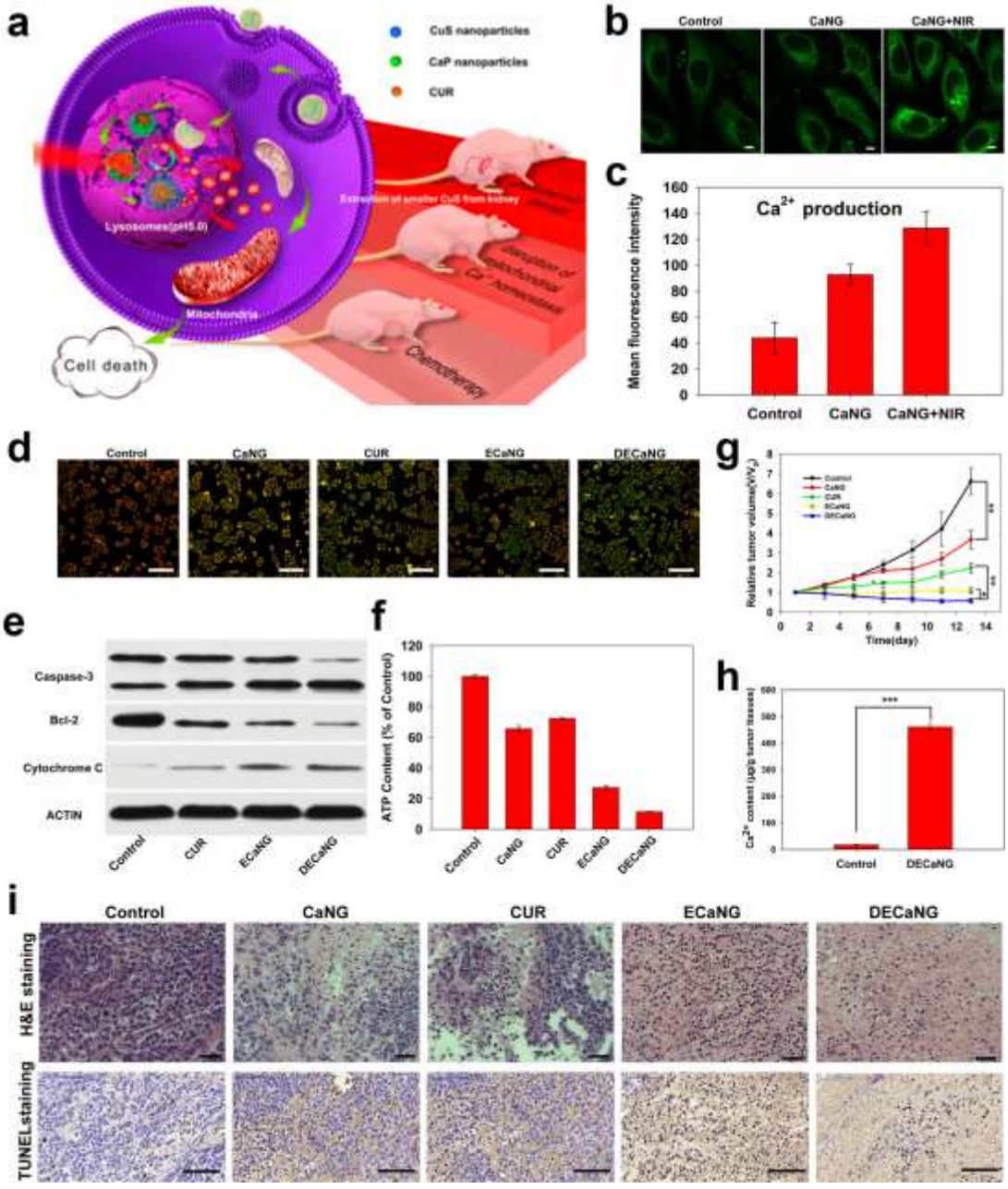

Figure 3. a) Schematic illustration of DECaNG-mediated Ca^{2+} overload and apoptosis; b,c) Increased Ca^{2+} level after the different treatments; d) Mitochondria membrane potential changes recorded by JC-1 staining; e) Western blot assays of intracellular caspase-3, Bcl-2, and cytochrome c; f) Intracellular ATP content change; g) Relative tumor volume changes with

different treatments; h) Ca^{2+} content in tumor tissues after treatment with DECaNG; i) H&E and TUNEL staining. Reproduced with permission.[43] Copyright 2018, American Chemical Society.

2.2 $CaCO_3$-based Nanomaterials

$CaCO_3$ is relatively stable in neutral and alkaline environments and is more easily decomposed into Ca^{2+} ions in acidic environments than CaP. Therefore, $CaCO_3$ is a suitable candidate as a Ca^{2+} resource to trigger Ca^{2+} overload in cancer cells. However, $CaCO_3$-mediated Ca^{2+} overload alone was unable to inhibit tumor growth effectively. To improve the therapeutic efficacy, some combined therapies based on $CaCO_3$-mediated Ca^{2+} overload have been proposed.[57,58] For example, liquid metal-glucose oxidase-$CaCO_3$ NPs (LMGC) were constructed, showing excellent efficacy in inhibiting tumor growth by the synergistic effect of Ca^{2+} overload, ATP generation inhibition, and photothermal effect.[59]

It is worth noting that the reason for the unsatisfied therapeutic effect on cancers treated with $CaCO_3$ NPs alone should be attributed to cellular self-regulation, which leads to the difficulty to increase the level of Ca^{2+} efficiently. Therefore, alternative approaches to disrupt Ca^{2+} homeostasis will be of help to increase the therapeutic outcome of Ca^{2+} overload. Similar to CaP, a phospholipid-coated amorphous $CaCO_3$ hybrid loaded with CUR (PL/ACC-CUR) was prepared to enhance Ca^{2+} overload by CUR-mediated Ca^{2+} efflux inhibition.[60] PL/ACC-CUR could specifically increase the intracellular Ca^{2+} level to cause Ca^{2+} overload and trigger mitochondria-related apoptosis in MCF-7 cells and inhibit tumor growth while sparing normal hepatocytes. In another study, anticancer cisplatin (CDDP) and CUR co-incorporated into $CaCO_3$ NPs as a multichannel Ca^{2+} nanomodulator were designed and obtained by a facile one-pot strategy by inducing multilevel destruction of mitochondria, exploiting the combined effects of Ca^{2+} burst release, Ca^{2+} efflux inhibition by CUR, and chemotherapeutic CDDP.[61] Interestingly, Zheng et al. found that $CaCO_3$/CUR nanoparticles can quickly cause mitochondrial Ca^{2+} overload and result in ROS increase, cytochrome C release, caspase-3 activation, gasdermin E cleavage, finally leading to pyrolysis and subsequent immune activation for immune therapy.[62]

Promoting Ca^{2+} influx is another strategy to enhance Ca^{2+} overload. It has been proved that kaempferol-3-O-rutinoside (KAE) shows an excellent anticancer activity due to its ability to disrupt calcium homeostasis and promote Ca^{2+} influx to fulfill Ca^{2+} overload-mediated cell apoptosis.[63] Therefore, the combination of $CaCO_3$ NPs and KAE is expected to display an efficiently synergistic Ca^{2+} overload effect. $CaCO_3$ NPs loaded with KAE and coated with

cancer cell membranes (M@$CaCO_3$@KAE NPs) were prepared to treat cancer by enhanced Ca^{2+} overload (**Figure 4**a).[64] The efficient Ca^{2+} overload-mediated by M@$CaCO_3$@KAE NPs can cause mitochondrial damage, oxidative stress, cytoskeleton collapse, and final apoptosis. The coating with the cancer cell membrane ensured the ability of tumor-targeting via innate properties of immune escape and aggregation. Compared to the use of $CaCO_3$ NPs alone, $CaCO_3$@KAE NPs could significantly improve the accumulation of Ca^{2+} (Figure 4b). Meanwhile, SERCA1 (Sarco(endo)plasmic Reticulum Ca^{2+}-ATPase Isoform 1) and PMCA4 (plasma membrane Ca^{2+}-ATPase), which are proteins related to calcium outflow, were down-regulated, while the pro-apoptotic protein CAMK4 (Ca^{2+}/calmodulin-dependent protein kinase) was up-regulated (Figure 4c).

Furthermore, M@$CaCO_3$@KAE NPs caused a decrease in the number of mitochondria, a mitochondrial membrane potential change, and mitochondrial lipid peroxidation (Figure 4d). As mitochondria are organelles responsible for cell energy supply, they play a crucial part in cellular cytoskeleton formation. When mitochondria are damaged, the cytoskeleton cannot form correctly (Figure 4e). As a consequence, the lamellipodium collapses and the structure of filopodia is modified, thus repressing the migration and invasion abilities of cancer cells and finally causing apoptosis. The membrane modification is the critical step to ensure that the M@$CaCO_3$@KAE NPs have the capacities for immune escape, thus avoiding the undesirable absorption at normal tissues.[65] By comparing the *in vivo* biodistribution of M@$CaCO_3$@KAE NPs with $CaCO_3$@KAE NPs, it was obvious that the membrane coating ensured enhanced targeting accumulation at the tumor sites. Therefore, M@$CaCO_3$@KAE NPs significantly enhanced tumor tissue Ca^{2+} overload *in vivo* (Figure 4f), and showed the highest efficacy of cancer therapy by causing a lot of cancer cell apoptosis and proliferation inhibition (Figure 4g and h). Besides, the expression of proliferation-related proteins (Ki67, PCNA, and BCL-2) was markedly restrained, while the apoptosis-related proteins (BAX, CAS3, and CAS9) were expressed at high levels. The expression of calcium outflow proteins (SERCA1 and PMCA4) decreased, and the level of the pro-apoptotic protein CAMK4 was significantly elevated. Meanwhile, Calpain1 was activated to achieve cytoskeleton degradation, similar to *in vitro* results. Interestingly, the natural non-toxic capsaicin (CAP), which is often used clinically to reduce inflammation and pain, has also been found to promote Ca^{2+} influx. Recently, Xu et al. designed $CaCO_3$@CAP NPs to achieve a highly therapeutic effect by simultaneously providing a TRPV1 channel activator (causing excessive Ca^{2+} influx) and exogenous Ca^{2+} to cause strong Ca^{2+} overload and cancer cell death (Figure 4i).[66] Finally, ovalbumin (OVA)@$CaCO_3$ NPs mediated Ca^{2+} overload can disrupt the autophagy inhibition condition in dendritic cells (DCs)

and improve DC maturation by enhanced DAMP (damage-associated molecular patterns) release from tumor cells, which offers an alternative strategy for improving cancer chemo-immunotherapy by the regulation of the intratumoral Ca^{2+}.[67]

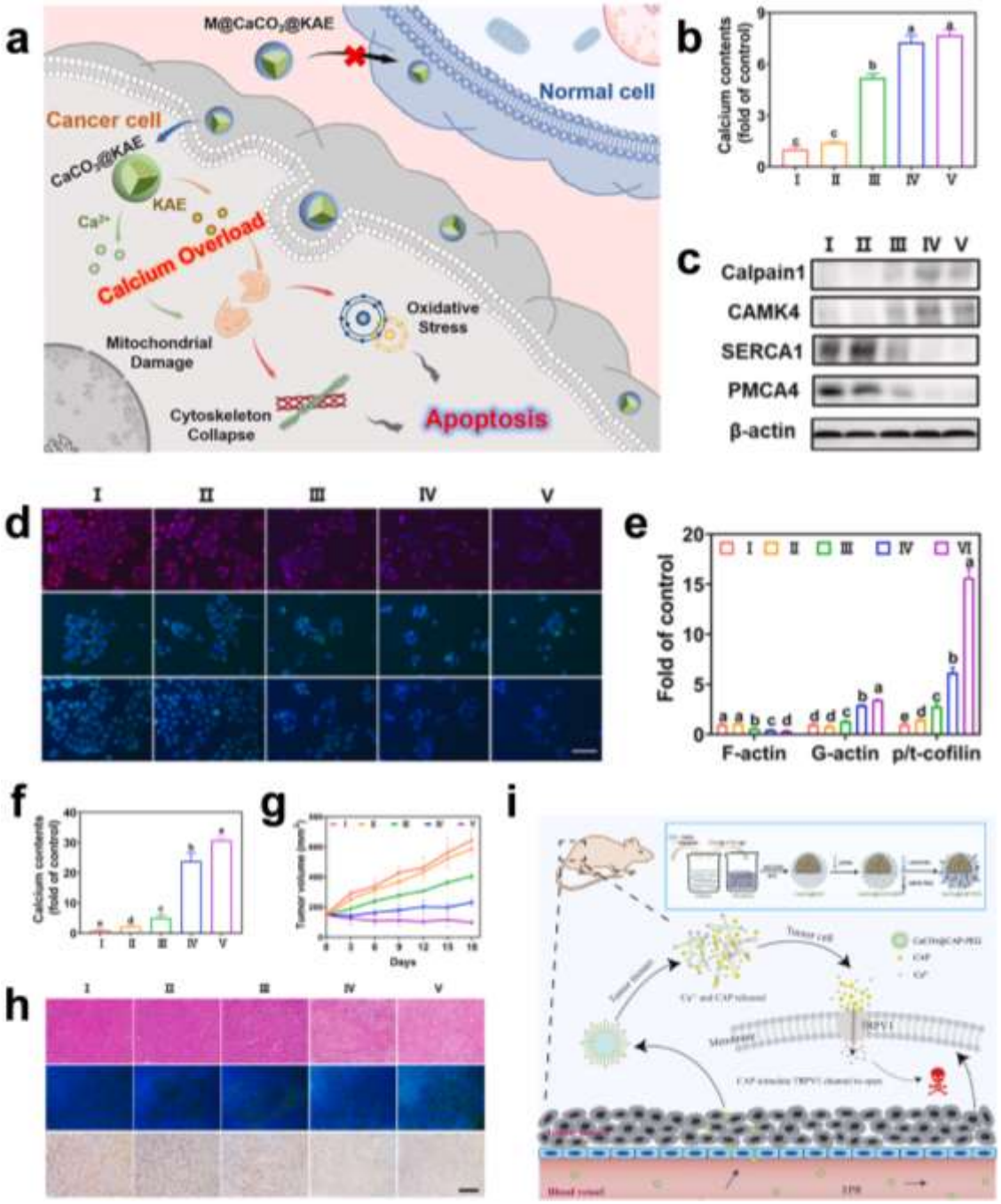

Figure 4. (a) Schematic illustration of M@$CaCO_3$@KAE NPs-mediated cancer therapy. (b) Ca^{2+} content changes. (c) Ca^{2+} regulated protein expression levels. (d) Effects on mitochondria. Top: Mitotracker staining for mitochondria number visualization; Middle: rhodamine 123 for mitochondrial membrane potential visualization; Bottom: nonyl acridine orange for mitochondrial lipid peroxidation. (e) The intensity of F-actin, G-actin, p-cofilin, and t-cofilin. (f) Tumor volume changes. (g) Ca^{2+} content change in tumor tissues. (h) H&E, TUNEL, and

Ki67 staining. I: Control; II: $CaCO_3$ NPs; III: KAE; IV: $CaCO_3$@KAE NPs; V: M@$CaCO_3$@KAE NPs. Reproduced with permission.[64] Copyright 2021, Elsevier Ltd. (i) Schematic illustration of $CaCO_3$@CAP NPs-mediated cancer therapy. Reproduced with permission.[66] Copyright 2022, Elsevier Ltd.

A recent study has evidenced that ultrasounds (US) can serve as an exogenously physical stimulus inducing Ca^{2+} overload through the upregulation of intracellular Ca^{2+} concentration by promoting Ca^{2+} influx from the extracellular fluid to the cytoplasm. Therefore, the US can enhance calcium-based nanomaterial-mediated Ca^{2+} overload. Zheng et al. developed CUR-incorporated $CaCO_3$ (CaCUR) NPs modified with poly(ethylene glycol) (^{PEG}CaCUR).[68] Dual US/CUR augmented mitochondrial Ca^{2+} overload induced immunogenic cell death (ICD) leading to an efficient immune response (**Figure 5**a), which also was observed in postoperative filler gel containing Ca^{2+} to prevent tumor recurrence and metastasis.[69] ^{PEG}CaCUR mediated Ca^{2+} overload reduced the mitochondrial membrane potential, further decreased by US treatment. Meanwhile, fewer mitochondria were observed in the ^{PEG}CaCUR group than in the control group, with the fewest detected in the ^{PEG}CaCUR+US group (Figure 5b). Therefore, ^{PEG}CaCUR associated with US stimulation can cause obvious mitochondrial damage and decrease mitochondrial production by enhanced Ca^{2+} overload. In addition, more calreticulin outside of the cell membrane appeared after ^{PEG}CaCUR+US treatment, and high-mobility group box 1 (HMGB1) and ATP showed significantly increased extracellular secretion. The above results confirmed that ^{PEG}CaCUR NPs with US treatment can induce stronger ICD. Efficient ICD promoted DC maturation and T cell activation. By the combination of Ca^{2+} overload and immune response activation, ^{PEG}CaCUR with US treatment could significantly inhibit the growth of tumors (Figure 5c), and a large number of cancer cells underwent apoptosis (Figure 5d), showing the high cancer treatment efficiency.

The disruption of the calcium buffering capacity to enhance Ca^{2+} overload by reactive oxygen species has been achieved recently.[70,71] A PEG-modified $CaCO_3$ nanoplatform loaded with a Ir(III) complex (IrCOOH-$CaCO_3$@PEG) was constructed for combined calcium overload and two-photon photodynamic therapy.[72] The generated $^1O_2$ during photodynamic reaction could cause calcium buffering capacity disruption, subsequently enhancing Ca^{2+} concentration. Similarly, $HO^{\bullet}$ from the Fenton-like reaction of $Co^{2+/3+}$ costituting a biodegradable chemodynamic therapeutic agent also showed inhibition on calcium buffering capacity enhancing Ca^{2+} overload. The additional intracellular Ca^{2+} promoted, in turn, hydroxyl radical accumulation.[73,74]

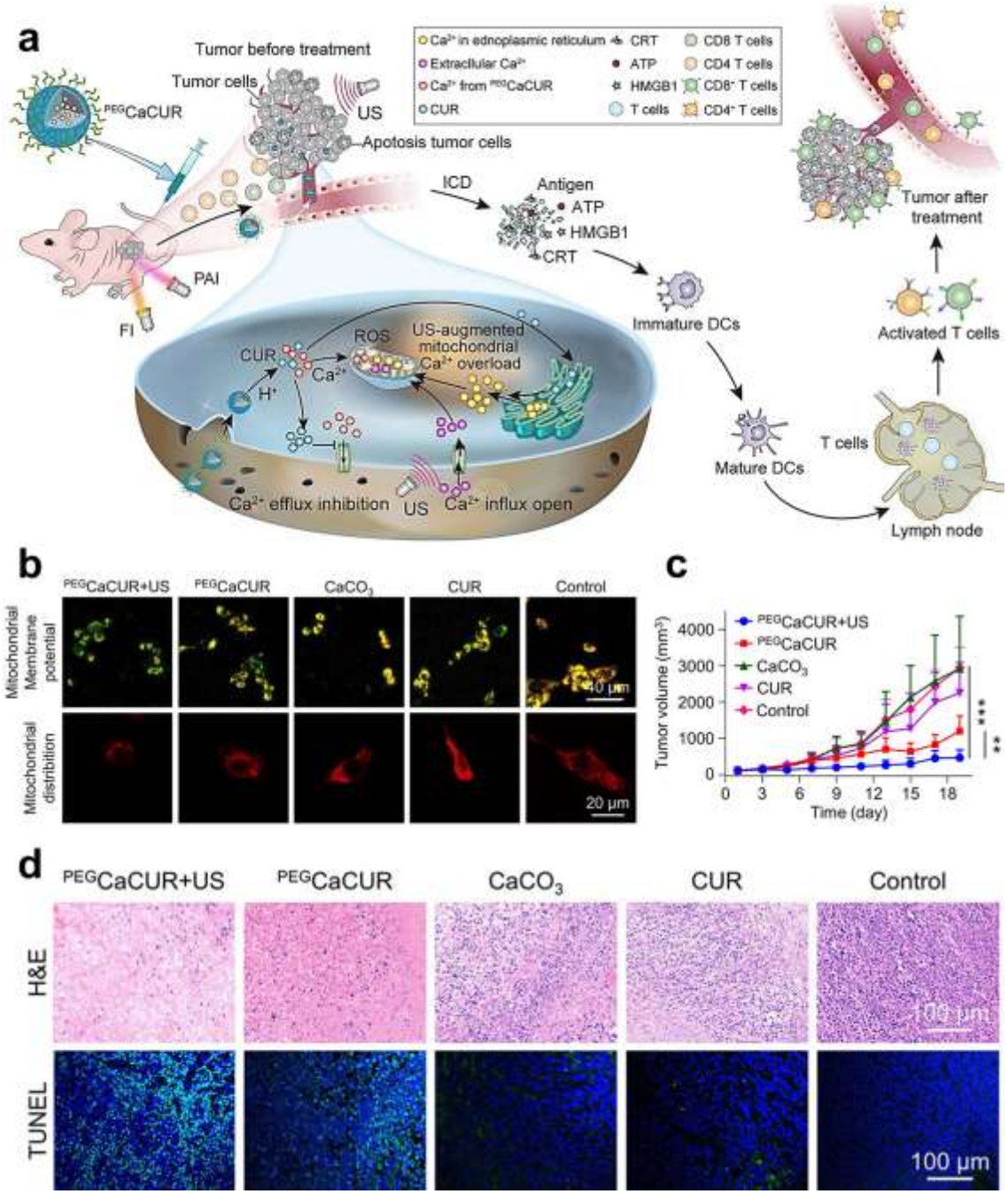

Figure 5. a) Schematic illustration of ^{PEG}CaCUR mediated Ca^{2+} overload and immune response activation; b) Effect of ^{PEG}CaCUR+US on mitochondria; c) Tumor volume changes; d) H&E and TUNEL staining. Reproduced with permission.[68] Copyright 2021, American Chemical Society.

2.3 CaO_2-based Nanomaterials

Compared with CaP and $CaCO_3$, CaO_2 NPs with lower stability cannot only generate Ca^{2+} but also H_2O_2 in the TME. leading to a direct increase of oxidative stress and higher mortality of cancer cells. Oxidative stress can cause Ca^{2+} influx into the cytoplasm from the extracellular

environment and ER or sarcoplasmic reticulum (SR) through the cell membrane and ER/SR channels, respectively.[75] Therefore, the increase of intracellular oxidative stress level can further disrupt the homeostasis of Ca^{2+} and enhance the Ca^{2+} overload, leading to intense cancer cell apoptosis.

Due to quick hydrolysis, surface modifications are necessary to endow CaO_2 with relatively high stability in body fluid and blood. To overcome this issue, sodium hyaluronate-modified CaO_2 NPs (SH-CaO_2) were prepared. SH-CaO_2 NPs can be easily and fast decomposed in an acid environment to produce abundant Ca^{2+} and H_2O_2, following to efficiently induce Ca^{2+} overload and cell death (**Figure 6**a and b).[76] The generated H_2O_2 can inhibit Ca^{2+} efflux, enhancing Ca^{2+} overload. After being treated with SH-CaO_2 NPs, ROS level and intracellular Ca^{2+} content remarkably increased. Moreover, the low expression of catalase in tumor cells can cause abnormal cellular H_2O_2 accumulation and an imbalanced calcium transport pathway, which are of help to guarantee an efficient Ca^{2+} overload (Figure 6c). Meanwhile, after the treatment with SH-CaO_2 NPs, the cell nucleus condensed and the mitochondrial activity drastically reduced. Furthermore, the enriched local concentration of Ca^{2+} increased the calcification around cancer cells, leading to tumor growth inhibition (Figure 6d). The *in vivo* results demonstrated that SH-CaO_2 NPs alone were very efficient against cancer, at a degree that was difficult to reach with CaP and $CaCO_3$, confirming the intrinsic advantage of using CaO_2. Interestingly, interference with Ca^{2+} overload can mediate M2-like tumor-associated macrophages (TAM) re-education and local Ca^{2+}-activated PD-L1 depletion for immunotherapy. In another study, An et al. designed DSPE-PEG2000 modified CaO_2 NPs loaded with a circular aptamer-DNAzyme complex (CaNP@cAD-PEG) to boost tumor immunotherapy.[77] CaNP@cAD-PEG were able to induce a significant Ca^{2+} interference effect and simultaneously reset TAM toward the M1 phenotype, by activating multiple inflammation-related signaling pathways and promoting in situ tumor-associated antigen release. The catalytic shear activity of cAD can be specifically activated by Ca^{2+}, reducing potential autoimmune disorders triggered by PD-L1 antibody. By synergistic effect, CaNP@cAD-PEG inhibited primary tumor growth and lung metastasis and showed a long-term immunological memory to prevent tumor recurrence. However, the direct effects of Ca^{2+} overload on NK cells and T cells still need further investigation. Alternatively, DOX was used in combination with ZIF-8 coated CaO_2 to treat cancer with higher efficacy exploiting the synergetic effect of mitochondrial Ca^{2+} overload-induced cell death and chemotherapy.[78]

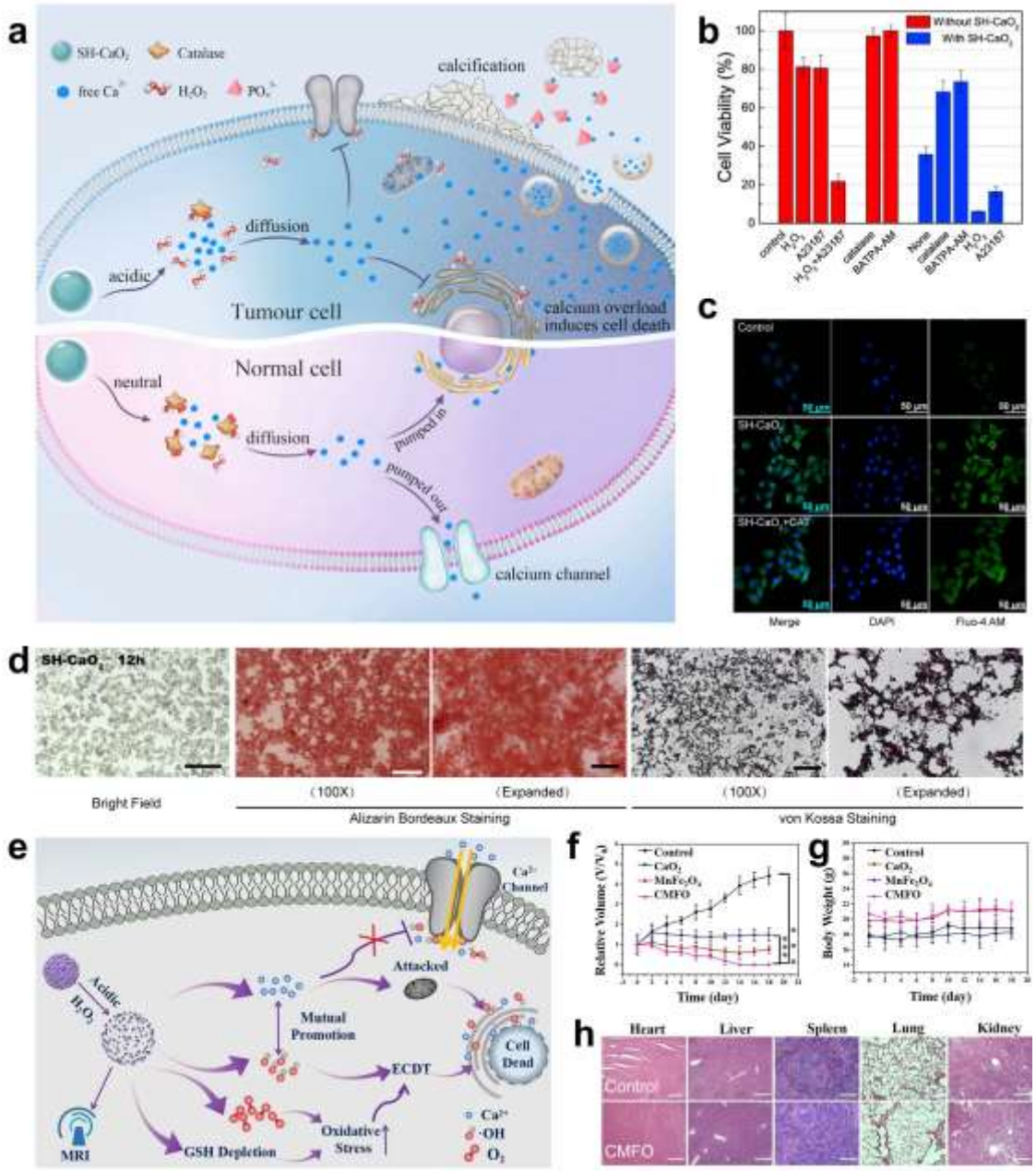

Figure 6. a) Schematic illustration of SH-CaO_2-mediated apoptosis; b) Cell viability assay. (c) Ca^{2+} content change after SH-CaO_2 NP treatment; d) Calcium mineralization. Reproduced with permission.[76] Copyright 2019, Elsevier Ltd. e) Synthesis process and spatially selective self-cascade catalyst mechanism of CMFO; f) Tumor volume changes after CMFO treatment; g) Body weight changes and h) H&E staining of the main organs. Reproduced with permission.[79] Copyright 2022, Elsevier Ltd.

Additionally, due to the high level of H_2O_2 produced by CaO_2, it is promising to combine Ca^{2+} overload with chemodynamic therapy (CDT), which utilizes Fenton or Fenton-like reactions to catalyze H_2O_2 into toxic hydroxyl radicals (HO•).[80-84] Therefore, a CaO_2 nanosystem coated by $MnFe_2O_4$ NPs (CMFO) as a protective umbrella was constructed to treat

cancer by the synergistic effect of Ca^{2+} overload and CDT mediated by Mn/Fe ions (Figure 6e).[79] CMFO was stable in normal tissues and could lead to a specific self-cascade catalytic reaction in tumor sites. Being cancer cells are more sensitive to Ca^{2+} in the presence of H_2O_2, the overloaded Ca^{2+} could induce apoptosis of tumor cells rather than in normal cells. By inhibiting the efflux and promoting the influx mediated by generated $HO^{\bullet}$, higher Ca^{2+} overload occurred, causing an efficient mitochondrial and cellular apoptosis. $MnFe_2O_4$ and H_2O_2 could also attenuate tumor hypoxia and deplete intracellular glutathione, amplifying oxidative stress and enhancing ROS-related activities. Based on these processes, the complete elimination of the tumor was achieved after CMFO treatment (Figure 6f), and CMFO showed low systemic toxicity and high biocompatibility (Figure 6g and h). Therefore, these "intelligent" and biodegradable CMFO NPs provide a new strategy for tumor-specific ROS-related treatment and spatially selective self-cascade synergistic therapy. Similarly, a cell membrane coated CaO_2@FePt-DOX@PDA (PDA, polydopamine) hybrid was developed for the combined application of chemotherapy, chemodynamic therapy, Ca^{2+} overload, amplified oxidative stress, and photothermal therapy. The combined FePt could convert H_2O_2 produced by CaO_2 into $HO^{\bullet}$, leading to enhanced apoptosis.[85] In another work, CaO_2 nanomaterials modified by Fe^{3+}/TA (tannic acid) polyphenol network were prepared to treat cancer by Ca^{2+} overload and CDT.[86,87] Notably, $HO^{\bullet}$ generated via the Fenton reaction desensitized the intracellular calcium ion proteins, promoting the occurrence of calcium overload and accelerating the death of cancer cells.

Because CaO_2 can also serve as a source of O_2, CaO_2-based composites were constructed by loading chlorin e6 (Ce6) to achieve a PDT. Shen et al. designed CaO_2@ZIF-Fe/Ce6@PEG (CaZFCP) to generate H_2O_2/O_2 self-supply and simultaneously Ca^{2+} overload in tumor cells for enhanced CDT/PDT.[88] To increase tissue penetration of light, up-conversion nanoparticles (UCNPs) were used as a template for the fabrication of UCNPs-Ce6@RuR (ruthenium red)@$mSiO_2$ NPs (UCRS) coated with HA and ε-polylysine (UCRSPH). The combined use of UCRSPH and stearic acid/HA modified CaO_2 showed great potential for highly specific, efficient combined therapy against tumor cells by integrating TME improvement, self-reinforcing PDT, and Ca^{2+} overload [89].

Similar to $CaCO_3$, CaO_2 can be combined with drugs able to further inhibit Ca^{2+} efflux and enhance Ca^{2+} overload. Transferrin (Tf) could be destroyed by H_2O_2 and could release Fe^{3+}, converting H_2O_2 into $HO^{\bullet}$ through the Fenton reaction.[90,91] Therefore, CUR and Tf co-loaded CaO_2 (CaO_2/Tf/CUR) NPs were formulated.[92] The cooperation of CUR and exogenous Ca^{2+} increased the intracellular Ca^{2+} level, reaching an efficient Ca^{2+} overload. Besides, Fe^{3+}

transformed H_2O_2 into $HO^{\bullet}$ and finally induced cancer cells apoptosis. Compared to the CaO_2 group without the drugs, a higher cellular uptake was observed with CaO_2 modified with Tf, confirming that Tf-conjugated NPs had a higher selectivity to cancer cells, via an endocytosis process mediated by the Tf receptor.[93] Cells treated with CaO_2/Tf/CUR NPs had the highest Ca^{2+} concentration among all groups, leading to efficient mitochondrial damage and apoptosis. *In vivo* results confirmed that CaO_2/Tf/CUR NPs possessed an excellent antitumor effect, with a lot of apoptotic cells identified in tumor tissues. Further, Transient Receptor Vanilloid 1 (TRPV1) thermal-sensitive cation channel can promote apoptosis by regulating Ca^{2+} influx after thermal activation (threshold ~43 °C).[94-96] NIR-responsive DPPC-DSPE-PEG2000-NH_2@PDPP@CaO_2@DOX NPs were designed.[97] Under NIR irradiation, the PTE promoted Ca^{2+} influx. Combined with Ca^{2+} release from CaO_2 by the acid response, efficient Ca^{2+} overload was achieved. Finally, breast cancer tumor growth was inhibited obviously by the combination of PTT, chemotherapy, and Ca^{2+} overload.

In addition, it has been confirmed that NO can promote the release of Ca^{2+} from ER by activating the opening of ryanodine receptors (RyRs).[98-101] Therefore, PDA-modified and arginine-loaded mesoporous CaO_2 NPs were designed.[102] H_2O_2 generated from CaO_2 can oxidize arginine to release locally NO. Subsequently, NO stimulates Ca^{2+} release. This Ca^{2+} together with the contribution of calcium from CaO_2 NP decomposition could synergistically and efficiently cause Ca^{2+} overload. By the combination of PTT, immune regulation, Ca^{2+} overload, and gas therapy, these NPs showed great potential to inhibit 4T1 tumor growth and formation of lung metastases.

2.4 Other Types of Ca^{2+}-based Nanomaterials

Recently, novel Ca^{2+}-based nanomaterials are emerging to enhance Ca^{2+} overload and promote cancer cell apoptosis. Hydrogen is an endogenous gas with high diffusibility and it has exhibited excellent antitumor performance as evidenced over the past decades.[103] Calcium hydride (CaH_2) NPs were designed for cancer treatment by combining the advantages of Ca^{2+} overload, TME modulation, and immune and hydrogen therapy (**Figure 7**a).[104] CaH_2 NPs can release abundant H_2, and change the pH into neutral or even alkaline from acid by the generated hydroxyl radicals. Compared with CaO, CaH_2 exhibited more serious toxicity and efficient apoptosis, which might be attributed to the combination of hydrogen and more effective Ca^{2+} overload (Figure 7b). Furthermore, CaH_2 caused more damages to mitochondria, and evidently decreased the generation of ATP compared with CaO (Figure 7c). As expected, the intracellular Ca^{2+} level increased after CaH_2 treatment rather than using CaO (Figure 7d). Interestingly,

CaH_2 NPs can also cause efficient ICD, which could activate T cells by antigen presentation (Figure 7e).

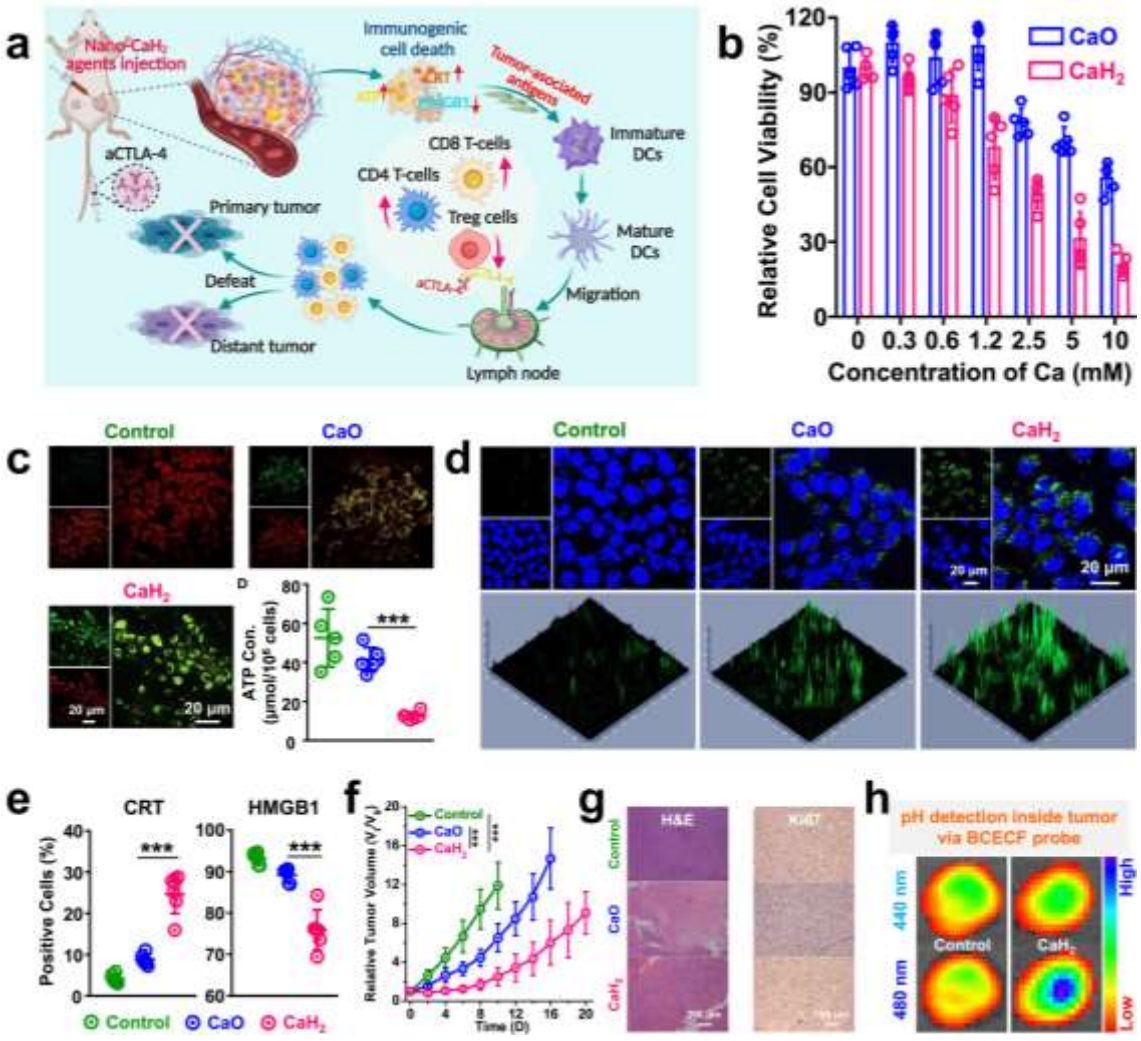

Figure 7. a) Schematic illustration of CaH_2 NPs mediating the synergistic effect of Ca^{2+} overload, TME regulation, and hydrogen-immune therapy; b) Cell viability. (c) Mitochondrial damage and ATP generation inhibition; d) Ca^{2+} content; e) ICD characterization; f) Tumor volume changes after CaH_2 and CaO treatment; g) H&E and Ki67 staining; h) pH value changes inside tumors. Reproduced with permission from Ref. [104]. Copyright 2022, Elsevier Ltd.

After being treated with CaH_2 *in vivo*, tumor growth was inhibited by the combination of Ca^{2+} overload, H_2 effect, microenvironment pH change, and activated immune responses (Figure 7f). A large population of apoptotic cancer cells appeared (Figure 7g) and the pH value inside the tumor increased (Figure 7h) after CaH_2 treatment. In addition, with the assistance of an immune checkpoint blockade (using an anti-T-lymphocyte-associated antigen 4 antibody, aCTLA-4), CaH_2 NPs showed higher efficacy in both primary and distant tumors. It was obvious that, in both tumors, the percentage of total T cell and cytotoxic T lymphocyte (CTL)

infiltration remarkably increased in the combination treatment group (CaH_2 NPs + aCTLA-4) compared with the CaH_2 NPs alone and the control groups. The combination treatment could greatly decrease the percentage of T_{reg} cells in the bilateral tumors, and also promote the polarization of macrophages from M2 to M1 type, favorable to achieving antitumor immunity. Therefore, while CaH_2 NPs could modulate the TME and induce cancer cell apoptosis to trigger CTL-mediated antitumor immunity, the CTLA-4 blockade could further enhance the systemic antitumor immune responses, bringing a better therapeutic effect.

H_2S is a molecular marker that regulates the activity of calcium channels.[105] It is well accepted that H_2S can down-regulate the permeability of Ca^{2+} channels, inhibiting Ca^{2+} efflux. Based on this evidence, CaS can serve as another ideal candidate to mediate H_2S-enhanced Ca^{2+} overload for cancer therapy. Zhao et al. designed a CaS-based nanosystem stabilized with PAA and zinc protoporphyrin (ZnPP@PAA-CaS) (**Figure 8**a).[106] ZnPP@PAA-CaS could release more Ca^{2+} and H_2S in the acidic microenvironment, revealing a notable clear acid-responsive decomposition ability (Figure 8b and c). As a consequence, Ca^{2+} overload was triggered while H_2S further enhanced intracellular Ca^{2+} level, seriously damaging the mitochondria, regulating cytoskeleton disassembly for cell division/migration inhibition, and causing cell apoptosis. Besides, the protective role of HO-1, a cytoprotective enzyme protecting the cancer cells from death induced by oxidative stress, could be repressed by ZnPP. Meanwhile, ZnPP@PAA-CaS NPs could cause ICD to inactivate T cells by DCs. The *in vivo* experiments demonstrated that ZnPP@PAA-CaS NPs could impede the growth of both primary tumors and distant metastases, and increase the survival rate of mice, especially with the assistance of αPD-1 (PD-1 antibody) (Figure 8d and e). Meanwhile, the main organs of mice treated with ZnPP@PAA-CaS NPs remained normal and all mice kept a regular body weight during treatments, indicating the high biosafety and biocompatibility of these NPs. In summary, the combination of ZnPP@PAA-CaS NPs mediated Ca^{2+} overload, H_2S therapy, protective pathway inhibition, and immunotherapy possesses a high efficiency for cancer therapy.

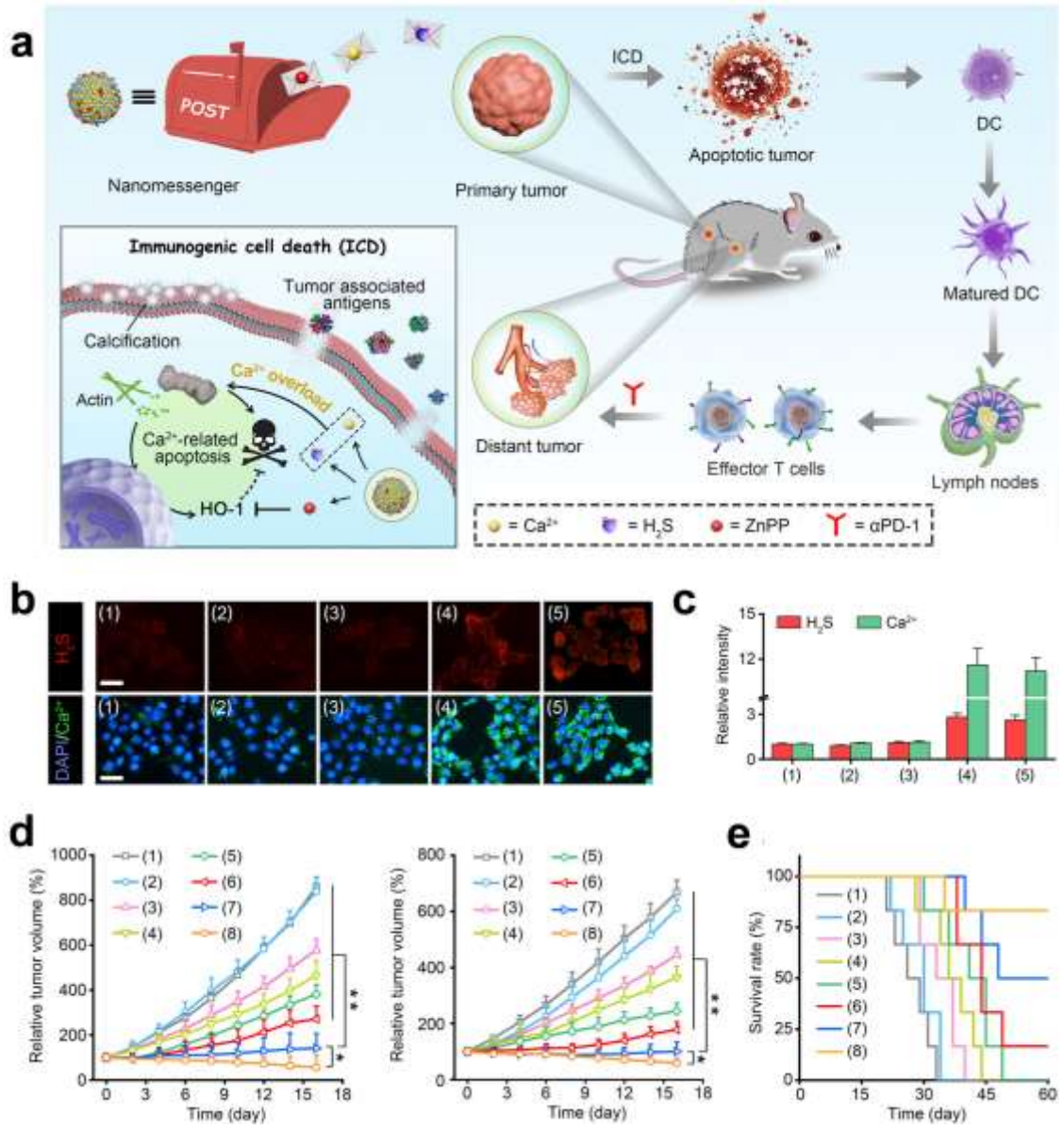

Figure 8. a) Schematic illustration of ZnPP@PAA-CaS mediated signaling cascade for antitumor immunotherapy; b,c) Intracellular H_2S and Ca^{2+} content change; d) Volume changes of primary and distant tumors; e) Survival curves of mice after the different treatments. In b and c, (1) blank; (2) PAA-Ca; (3) ZnPP; (4) PAA-CaS; (5) ZnPP@PAA-CaS. In d and e, (1) blank; (2) PAA-Ca; (3) ZnPP; (4) αPD-1; (5) PAA-CaS; (6) ZnPP@PAA-CaS; (7) PAA-CaS + αPD-1; (8) ZnPP@PAA-CaS + αPD-1. Reproduced with permission from ref. 83. Copyright 2021, American Chemical Society.

3. Perspectives

In this review, different types of Ca^{2+}-based nanomaterials for cancer therapy have been summarized, and the strategies to enhance Ca^{2+} overload discussed. Besides $CaCO_3$, CaO_2, and CaP, which have been widely studied, some new Ca^{2+}-based nanomaterials are also emerging,

such as CaH_2 and CaS. All of them result in a promising platform for Ca^{2+} overload-based cancer therapy. Nevertheless, Ca^{2+} overload-mediated cancer therapy remains in its infancy, and more endeavors are urgently needed to address some limitations (such as low cellular uptake of nanomaterials, slow Ca^{2+} release, and the inhibition of Ca^{2+} overload by homeostasis regulation) to further improve the performance and obtain the satisfactory efficiency. Meanwhile, the clinical translation of Ca^{2+}-based nanomaterials faces three main challenges. First, the enrichment efficiency of Ca^{2+}-based nanomaterials in tumor sites is still low after intravenous injection. Second, the efficiency of monotherapy by Ca^{2+} overload still needs to be improved. Third, the long-term biosafety of Ca^{2+}-based nanomaterials needs to be confirmed, although the short-term biosafety is satisfactory. It is worth noting that when the concentration of intracellular increases to 1.5-2 folds, apoptosis is triggered and the tumors start to be inhibited to a certain extent.[38,41,43,59,64,68] Interestingly, once the concentration of the intracellular Ca^{2+} exceeds 10 folds, significant apoptosis happens and the tumor can be inhibited efficiently.[76,79,104,106]

Generally, the rate of cellular uptake of nanomaterials deserves further optimization, necessary not only for Ca^{2+} overload-mediated cancer therapy but for most nanomedicine therapies such as PTT, PDT, and CDT. Indeed, the prerequisite of obtaining a satisfactory curative effect is delivering enough synthesized NPs into cancer cells while avoiding uptake by normal cells. The surface modification of nanomaterials has shown great potential to enhance nanomaterials' internalization and obtain targeting capability. HA, FA, erythrocyte membrane, and homologous cancer cell membrane are currently common choices. Meanwhile, enhancing the uptake capacity (via phagocytosis or pinocytosis) is an alternative strategy.[107-110] For example, Hou et al. designed a hollow mesoporous nanoplatform made of Prussian blue NPs encapsulating idrossiclorochina and coated with mannose for cancer therapy, which can facilitate cellular internalization via sugar receptor-mediated endocytosis.[111] while Han et al. used cationic liposomes constituted of oleic acid, a collagen mimetic cleavable lipopeptide, and glutamate-rich segment to enhance endocytosis through surface charge reversal in response to matrix metallopeptidase 9.[112] Furthermore, the shape of nanomaterials allows to also control of the uptake rate and targeting capability. Cong et al. demonstrated that mesoporous silica nanorods can be taken up by cancer cells more efficiently than nanospheres, while the metabolism and endocytosis of nanorods were suppressed in healthy cells.[113] Moreover, the surface modification and the morphological regulation also endow Ca^{2+}-based nanomaterials with the ability to better target cancer cells rather than normal cells, which is beneficial to improve biosafety and promote further clinical applications. However, there are no detailed

studies about the effect of the shape of Ca^{2+}-based nanomaterials on triggering intracellular Ca^{2+} overload yet, which needs more effort and attention to uncovering this relation. Meanwhile, the enhanced permeability and retention effect and transcytosis bring Ca^{2+}-based nanomaterials to the tumor sites, reducing the potential side effects on normal tissues.[114,115] Furthermore, how to inhibit the exocytosis of Ca2+-based nanomaterials after internalization by cancer cells and related studies to get an effective therapeutic strategy are still lacking. Promoting Ca^{2+} release after the uptake of nanomaterials is also pivotal for cancer therapy exploiting Ca^{2+} overload. Varied Ca^{2+}-based nanomaterials of different natures and compositions show different abilities to trigger Ca^{2+} overload. Due to the high stability and the slow release of Ca^{2+}, CaP nanomaterials alone usually cause a weak Ca^{2+} overload. $CaCO_3$ has a rapidly acid response to release more Ca^{2+}. With the increase in solubility, CaO_2, CaS, and CaH_2 particles will easily release high doses of Ca^{2+}. However, to maintain the stability of Ca^{2+}-based nanomaterials before entering the cells, appropriate surface modifications are required. Meanwhile, varied methods have been developed to accelerate the dissolution of Ca^{2+}-based nanomaterials and Ca^{2+} release. As discussed above, CuS-mediated PTT could accelerate Ca^{2+} release from tricalcium phosphate nanoparticles. Efficient decomposition of Ca^{2+}-based nanomaterials in cancer cells can be considered an efficient way to increase the level of Ca^{2+}. Therefore, increasing the content of H^+ will promote the degradation of Ca^{2+}-based nanomaterials due to the acid response, triggering a rapid release of Ca^{2+}. Glucose oxidase catalyzes the transformation of glucose into gluconic acid and hydrogen peroxide, enhancing the intracellular acidity of cancer cells.[116,117] A liquid metal-glucose oxidase-$CaCO_3$ composite was prepared, endowed with the capacity to accelerate the release of Ca^{2+} by gluconic acid.[59] It is well known that self-regulation of Ca^{2+} homeostasis is the main barrier to efficient Ca^{2+} overload.[118-121] This process can be broken by inducing Ca^{2+} release from ER, promoting Ca^{2+} influx, and inhibiting Ca^{2+} efflux. ER is the intracellular Ca^{2+} storage organelle and can regulate intracellular Ca^{2+} concentration. Some molecules, such as ionafarnib, can activate caspase family proteins which can trigger ER stress to release Ca^{2+}.[122] Meanwhile, Ca^{2+} channel inhibitors (e.g., CUR or T-type calcium channel blockers) have been used to hamper the efflux of Ca^{2+}.[68,123] Furthermore, NO also could stimulate Ca^{2+} release from ER by activating the opening cellular channels, leading to intracellular Ca^{2+} overload.[102] Some methods to promote Ca^{2+} influx have also been exploited. KAE and CAP are efficient regulators for Ca^{2+} influx promotion.[64,66] Alternatively, ultrasound as an exogenously physical stimulus has been used to induce Ca^{2+} influx.[68] Interestingly, hydrogen peroxide and hydroxyl radicals have displayed the dual abilities to promote influx and inhibit efflux of Ca^{2+},[75,76,79] while H_2S was recently

found to be able to down-regulate the permeability of the Ca^{2+} channel and inhibit Ca^{2+} efflux.[106] Another potential way to interfere with Ca^{2+} homeostasis is curtailing the conduction due to the excess of Ca^{2+}.[1,4,11,13] Varieties of signaling molecules are needed to maintain Ca^{2+} homeostasis. Therefore, antagonizing the conduction way of Ca^{2+} is helpful to induce continuous Ca^{2+} overload. Naturally, the combination of enhanced endocytosis, Ca^{2+} efflux inhibition, Ca^{2+} efflux promotion, triggering Ca^{2+} release from ER, and accelerated Ca^{2+} release from nanomaterials can further enhance the Ca^{2+} overload to obtain a better therapeutic effect. Moreover, Ca^{2+}-based nanomaterials prepared from soluble calcium salts (such as $CaCl_2$, $CaBr_2$, $Ca(NO_3)_2$, calcium aspartate, and calcium gluconate) for Ca^{2+} overload-mediated cancer therapy by suitable surface modification and encapsulation (referring to the preparation of NaCl NPs) will be an attractive choice to cause Ca^{2+} burst.[124,125]

One point that needs to be emphasized is that once cancer cell apoptosis happened, the intracellular Ca^{2+} would be released into the environment and then diffuses into the surrounding. It was repoted that the extracellular concentration of Ca^{2+} is ~1300 times that of the intracellular calcium concentration (~100 nM).[126] Therefore, there is only a slight increase in the extracellular Ca^{2+} concentration after cancer cell apoptosis. The slight increase of extracellular Ca^{2+} concentration does not damage normal cells and tissues, but promotes tissue regeneration, especially in bone repair. Indeed, varied Ca^{2+}-based scaffolds and hydrogels have been developed for bone tissue engineering by releasing Ca^{2+} to stimulate osteogenic differentiation and mineralization.[127-132]

In summary, in the arena of fighting against cancer, Ca^{2+}-based nanomaterials and Ca^{2+} overload cancer therapies are demonstrating their distinctive power. The variety of enhancement strategies for Ca^{2+} overload can promote a better design of Ca^{2+}-based functional nanomaterials. It is expected that this review provides practical assistance for the utilization of Ca^{2+} overload and inspires the development of new tumor treatments.

Acknowledgements

The authors greatly acknowledge the financial support from the National Natural Science Foundation of China (No. 82100974), Shandong Province Major Scientific and Technical Innovation Project (No. 2021SFGC0502), Shandong Province Key Research and Development Program (No. 2021ZDSYS18), Shandong Province Natural Science Foundation (ZR2021QH241 and ZR202102180927), Qilu Young Scholars Program of Shandong University. This work was supported by the Interdisciplinary Thematic Institute SysChem via the IdEx Unistra (ANR-10-IDEX-0002) within the program Investissement d'Avenir. We also

wish to acknowledge the Centre National de la Recherche Scientifique (CNRS) and the International Center for Frontier Research in Chemistry (icFRC). Figure 1 and ToC figure were partly from Servier Medical Art with some modification (http://smart.servier.com/), licensed under a Creative Common Attribution 3.0 Generic License (https://creativecommons.org/licenses/by/3.0/).

Conflict of Interest

The authors declare no conflict of interest.

References

[1] C. Giorgi, S. Marchi, P. Pinton, *Nat. Rev. Mol. Cell Biol.* **2018**, *19*, 713.

[2] M. Kerkhofs, M. Bittremieux, G. Morciano, C. Giorgi, P. Pinton, J. B. Parys, G. Bultynck, *Cell Death Dis.* **2018**, *9*, 1.

[3] J. Soboloff, B. S. Rothberg, M. Madesh, D. L. Gill, *Nat. Rev. Mol. Cell Bio.* **2012**, *13*, 549.

[4] M. Trebak, J.-P. Kinet, *Nat. Rev. Immunol.* **2019**, *19*, 154.

[5] J. D. Thatcher, *Sci. Signal.* **2010**, *3*, tr3.

[6] M. Malek, A. M. Wawrzyniak, P. Koch, C. Lüchtenborg, M. Hessenberger, T. Sachsenheimer, W. Jang, B. Brügger, V. Haucke, *Nat. Commun.* **2021**, *12*, 1.

[7] L. Marongiu, F. Mingozzi, C. Cigni, R. Marzi, M. Di Gioia, M. Garrè, D. Parazzoli, L. Sironi, M. Collini, R. Sakaguchi, *Sci. Signal.* **2021**, *14*, eaaz2120.

[8] J. Loncke, A. Kaasik, I. Bezprozvanny, J. B. Parys, M. Kerkhofs, G. Bultynck, *Trends Cell Biol.* **2021**, *31*, 598.

[9] J. Rieusset, *Cell Death Dis.* **2018**, *9*, 1.

[10] C. Cardenas, A. Lovy, E. Silva-Pavez, F. Urra, C. Mizzoni, U. Ahumada-Castro, G. Bustos, F. Jaňa, P. Cruz, P. Farias, *Sci. Signal.* **2020**, *13*, eaay1212.

[11] C. Giorgi, A. Danese, S. Missiroli, S. Patergnani, P. Pinton, *Trends Cell Biol.* **2018**, *28*, 258.

[12] D. E. Clapham, *Cell* **2007**, *131*, 1047.

[13] S. Marchi, S. Patergnani, S. Missiroli, G. Morciano, A. Rimessi, M. R. Wieckowski, C. Giorgi, P. Pinton, *Cell Calcium* **2018**, *69*, 62.

[14] M. W. Berchtold, H. Brinkmeier, M. Muntener, *Physiol. Rev.* **2000**, *80*, 1215.

[15] J. H. Choi, S. Y. Jeong, M. R. Oh, P. D. Allen, E. H. Lee, *Cells* **2020**, *9*, 850.

[16] J. Hartmann, R. M. Karl, R. P. Alexander, H. Adelsberger, M. S. Brill, C. Rühlmann, A. Ansel, K. Sakimura, Y. Baba, T. Kurosaki, *Neuron* **2014**, *82*, 635.

[17] J. S. Dittman, T. A. Ryan, *Nat. Rev. Neurosci.* **2019**, *20*, 177.

[18] D. R. Green, G. Kroemer, *Science* **2004**, *305*, 626.

[19] M. Fan, J. Zhang, C.-W. Tsai, B. J. Orlando, M. Rodriguez, Y. Xu, M. Liao, M.-F. Tsai, L. Feng, *Nature* **2020**, *582*, 129.

[20] L. Jiao, M. Li, Y. Shao, Y. Zhang, M. Gong, X. Yang, Y. Wang, Z. Tan, L. Sun, L. Xuan, *Cell Death Dis.* **2019**, *10*, 1.

[21] S. Kuchay, C. Giorgi, D. Simoneschi, J. Pagan, S. Missiroli, A. Saraf, L. Florens, M. P. Washburn, A. Collazo-Lorduy, M. Castillo-Martin, *Nature* **2017**, *546*, 554.

[22] J. S. Bayley, C. B. Winther, M. K. Andersen, C. Grønkjær, O. B. Nielsen, T. H. Pedersen, J. Overgaard, *P. Natl. Acad. Sci. USA* **2018**, *115*, E9737.

[23] E. Norberg, V. Gogvadze, M. Ott, M. Horn, P. Uhlen, S. Orrenius, B. Zhivotovsky, *Cell Death Dis.* **2008**, *15*, 1857.

[24] J. Ha, D. Lee, S.-H. Lee, C.-O. Yun, Y.-C. Kim, *Biomaterials* **2019**, *197*, 51.

[25] D. Bano, J. H. Prehn, *EBioMedicine* **2018**, *30*, 29.

[26] J. Hamilton, T. Brustovetsky, N. Brustovetsky, *J. Biol. Chem.* **2021**, *296*, 100669.

[27] S. Malyala, Y. Zhang, J. O. Strubbe, J. N. Bazil, *PLoS Comput. Biol.* **2019**, *15*, e1006719.

[28] Y. Liu, M. Zhang, W. Bu, *View* **2020**, *1*, e18.

[29] C. Qi, J. Lin, L.-H. Fu, P. Huang, *Chem. Soc. Rev.* **2018**, *47*, 357.

[30] S. Bai, Y. Lan, S. Fu, H. Cheng, Z. Lu, G. Liu, *Nano-Micro Lett.* **2022**, *14*, 145.

[31] J. Yao, H. Peng, Y. Qiu, S. Li, X. Xu, A. Wu, F. Yang, *J. Mater. Chem. B* **2022**, *10*, 1508.

[32] R. Khalifehzadeh, H. Arami, *Adv. Colloid Interface Sci.* **2020**, *279*, 102157.

[33] R. Z. LeGeros, *Chem, Rev.* **2008**, *108*, 4742.

[34] J. Tang, C. B. Howard, S. M. Mahler, K. J. Thurecht, L. Huang, Z. P. Xu, *Nanoscale* **2018**, *10*, 4258.

[35] M. Du, J. Chen, K. Liu, H. Xing, C. Song, *Compos. Part B-Eng.* **2021**, *215*, 108790.

[36] X. Li, L. Wei, J. Li, J. Shao, B. Yi, C. Zhang, H. Liu, B. Ma, S. Ge, *Appl. Mater. Today* **2021**, *22*, 100942.

[37] Y. Shen, F. Liu, J. Duan, W. Wang, H. Yang, Z. Wang, T. Wang, Y. Kong, B. Ma, M. Hao, *Nano Lett.* **2021**, *21*, 7371.

[38] Y. Sun, Y. Chen, X. Ma, Y. Yuan, C. Liu, J. Kohn, J. Qian, *ACS Appl. Mater. Interfaces* **2016**, *8*, 25680.

[39] J. W. Liu, Y. G. Yang, K. Wang, G. Wang, C. C. Shen, Y. H. Chen, Y. F. Liu, T. D. James, K. Jiang, H. Zhang, *ACS Appl. Mater. Interfaces* **2021**, *13*, 3669.

[40] S. Zhang, X. Ma, D. Sha, J. Qian, Y. Yuan, C. Liu, *J. Mater. Chem. B* **2020**, *8*, 9589.

[41] M. Xiaoyu, D. Xiuling, Z. Chunyu, S. Yi, Q. Jiangchao, Y. Yuan, L. Changsheng, *Nanoscale* **2019**, *11*, 15312.

[42] J. Liu, C. Zhu, L. Xu, D. Wang, W. Liu, K. Zhang, Z. Zhang, J. Shi, *Nano Lett.* **2020**, *20*, 8102.

[43] L. Xu, G. Tong, Q. Song, C. Zhu, H. Zhang, J. Shi, Z. Zhang, *ACS Nano* **2018**, *12*, 6806.

[44] R. Sharma, A. Gescher, W. Steward, *Eur. J. Cancer* **2005**, *41*, 1955.

[45] L. Guo, D. D. Yan, D. Yang, Y. Li, X. Wang, O. Zalewski, B. Yan, W. Lu, *ACS Nano* **2014**, *8*, 5670.

[46] X. Liu, F. Fu, K. Xu, R. Zou, J. Yang, Q. Wang, Q. Liu, Z. Xiao, J. Hu, *J. Mater. Chem. B* **2014**, *2*, 5358.

[47] M. Xuan, Z. Wu, J. Shao, L. Dai, T. Si, Q. He, *J. Am. Chem. Soc.* **2016**, *138*, 6492.

[48] M. Shui, Y. Sun, Z. Zhao, K. Cheng, Y. Xiong, Y. Wu, W. Fan, J. Yu, Y. Yan, Z. Yang, *Optik* **2013**, *124*, 6115.

[49] J. Chen, M. Qiu, S. Zhang, B. Li, D. Li, X. Huang, Z. Qian, J. Zhao, Z. Wang, D. Tang, *J. Colloid Interf. Sci.* **2022**, *605*, 263.

[50] T. Pan, W. Fu, H. Xin, S. Geng, Z. Li, H. Cui, Y. Zhang, P. K. Chu, W. Zhou, X. F. Yu, *Adv. Funct. Mater.* **2020**, *30*, 2003069.

[51] J. Li, B. Qu, Q. Wang, X. Ning, S. Ren, C. Liu, R. Zhang, *ACS Appl. Nano Mater.* **2022**, *5*, 7733.

[52] M. Qiu, J. Chen, X. Huang, B. Li, S. Zhang, P. Liu, Q. Wang, Z. R. Qian, Y. Pan, Y. Chen, J. Zhao, *ACS Appl. Mater. Interfaces* **2022**, *14*, 21954.

[53] M.-F. Wei, M.-W. Chen, K.-C. Chen, P.-J. Lou, S. Y.-F. Lin, S.-C. Hung, M. Hsiao, C.-J. Yao, M.-J. Shieh, *Autophagy* **2014**, *10*, 1179.

[54] S.-S. Wan, L. Zhang, X.-Z. Zhang, *ACS Central Sci.* **2019**, *5*, 327.

[55] L. Shao, Y. Li, F. Huang, X. Wang, J. Lu, F. Jia, Z. Pan, X. Cui, G. Ge, X. Deng, Y. Wu, *Theranostics* **2020**, *10*, 7273.

[56] X. Wang, Y. Li, X. Deng, F. Jia, X. Cui, J. Lu, Z. Pan, Y. Wu, *ACS Appl. Mater. Interfaces* **2021**, *13*, 39112.

[57] M. Yao, W. Han, L. Feng, Z. Wei, Y. Liu, H. Zhang, S. Zhang, *Eur. J. Med. Chem.* **2022**, *233*, 114236.

[58] C. Xie, T. Zhang, Y. Fu, G. Han, X. Li, *Nano Res.* **2022**, *15*, 8281.

[59] X. L. Ding, M. D. Liu, Q. Cheng, W. H. Guo, M. T. Niu, Q. X. Huang, X. Zeng, X. Z. Zhang, *Biomaterials* **2022**, *281*, 121369.

[60] C. Wang, F. Yu, X. Liu, S. Chen, R. Wu, R. Zhao, F. Hu, H. Yuan, *Adv. Healthc. Mater.* **2019**, *8*, 1900501.

[61] P. Zheng, B. Ding, R. Shi, Z. Jiang, W. Xu, G. Li, J. Ding, X. Chen, *Adva. Mat.* **2021**, *33*, 2007426.

[62] P. Zheng, B. Ding, G. Zhu, C. Li, J. Lin, *Angew. Chem. Int. Ed.* **2022**, *61*, e202204904.

[63] Y. Li, X. Yu, Y. Wang, X. Zheng, Q. Chu, *Food Funct.* **2021**, *12*, 8351.

[64] Y. Li, S. Zhou, H. Song, T. Yu, X. Zheng, Q. Chu, *Biomaterials* **2021**, *277*, 121080.

[65] Q. Chu, H. Zhu, B. Liu, G. Cao, C. Fang, Y. Wu, X. Li, G. Han, *J. Mater. Chem. B* **2020**, *8*, 8546.

[66] M. Xu, J. Zhang, Y. Mu, M. F. Foda, H. Han, *Biomaterials* **2022**, *284*, 121520.

[67] J. An, K. Zhang, B. Wang, S. Wu, Y. Wang, H. Zhang, Z. Zhang, J. Liu, J. Shi, *ACS Nano* **2020**, *14*, 7639.

[68] P. Zheng, B. Ding, Z. Jiang, W. Xu, G. Li, J. Ding, X. Chen, *Nano Lett.* **2021**, *21*, 2088.

[69] D. Cao, W. Guo, C. Cai, J. Tang, W. Rao, Y. Wang, Y. Wang, L. Yu, J. Ding, *Adv. Funct. Mater.* **2022**, 2206084.

[70] J. Zhu, A. Jiao, Q. Li, X. Lv, X. Wang, X. Song, B. Li, Y. Zhang, X. Dong, *Acta Biomater.* **2022**, *137*, 252.

[71] X. Huang, M. Qiu, T. Wang, B. Li, S. Zhang, T. Zhang, P. Liu, Q. Wang, Z. R. Qian, C. Zhu, M. Wu, J. Zhao, *J. Nanobiotechnol.* **2022**, *20*, 93.

[72] J. Shen, X. Liao, W. Wu, T. Feng, J. Karges, M. Lin, H. Luo, Y. Chen, H. Chao, *Inorg. Chem. Front.* **2022**, *9*, 4171.

[73] X. Zhao, X. Wan, T. Huang, S. Yao, S. Wang, Y. Ding, Y. Zhao, Z. Li, L. Li, *J. Colloid Interf. Sci.* **2022**, *618*, 270.

[74] W. Xie, J. Ye, Z. Guo, J. Lu, W. Xu, X. Gao, H. Huang, R. Hu, L. Mao, Y. Wei, L. Zhao, *Chem. Eng. J.* **2022**, *438*, 135372.

[75] G. Ermak, K. J. Davies, *Mol. Immunol* **2002**, *38*, 713.

[76] M. Zhang, R. Song, Y. Liu, Z. Yi, X. Meng, J. Zhang, Z. Tang, Z. Yao, Y. Liu, X. Liu, *Chem* **2019**, *5*, 2171.

[77] J. An, M. Liu, L. Zhao, W. Lu, S. Wu, K. Zhang, J. Liu, Z. Zhang, J. Shi, *Adv. Funct. Mater.* **2022**, 2201275.

[78] Q. Sun, B. Liu, R. Zhao, L. Feng, Z. Wang, S. Dong, Y. Dong, S. Gai, H. Ding, P. Yang, *ACS Appl. Mater. Interfaces* **2021**, *13*, 44096.

[79] X. Wang, C. Li, H. Jin, X. Wang, C. Ding, D. Cao, L. Zhao, G. Deng, J. Lu, Z. Wan, X. Liu, *Chem. Eng. J.* **2022**, *432*, 134438.

[80] S. Xie, W. Sun, C. Zhang, B. Dong, J. Yang, M. Hou, L. Xiong, B. Cai, X. Liu, W. Xue, *ACS Nano* **2021**, *15*, 7179.

[81] C. He, X. Zhang, C. Chen, X. Liu, Y. Chen, R. Yan, T. Fan, Y. Gai, R. J. Lee, X. Ma, *Acta Biomater.* **2021**, *122*, 354.

[82] Q. Chen, D. Yang, L. Yu, X. Jing, Y. Chen, *Mater. Horiz.* **2020**, *7*, 317.

[83] B. Ma, S. Wang, F. Liu, S. Zhang, J. Duan, Z. Li, Y. Kong, Y. Sang, H. Liu, W. Bu, *J. Am. Chem. Soc.* **2019**, *141*, 849.

[84] B. Ma, Y. Nishina, A. Bianco, *Carbon* **2021**, *178*, 783.

[85] F. Zhang, C. Xin, Z. Dai, H. Hu, Q. An, F. Wang, Z. Hu, Y. Sun, L. Tian, X. Zheng, *ACS Appl. Mater. Interfaces* **2022**, *14*, 40633.

[86] J. Liu, Y. Jin, Z. Song, L. Xu, Y. Yang, X. Zhao, B. Wang, W. Liu, K. Zhang, Z. Zhang, *Chem. Eng. J.* **2021**, *411*, 128440.

[87] F. Chen, B. Yang, L. Xu, J. Yang, J. Li, *ChemMedChem* **2021**, *16*, 2278.

[88] J. Shen, H. Yu, Y. Shu, M. Ma, H. Chen, *Adv. Funct. Mater.* **2021**, *31*, 2106106.

[89] Y. Jiang, W. Meng, L. Wu, K. Shao, L. Wang, M. Ding, J. Shi, X. Kong, *Adv. Healthc. Mater.* **2021**, *10*, 2100789.

[90] H. Kawabata, *Free Radical Bio. Med.* **2019**, *133*, 46.

[91] K. Fan, X. Jia, M. Zhou, K. Wang, J. o. Conde, J. He, J. Tian, X. Yan, *ACS Nano* **2018**, *12*, 4105.

[92] Y. Yin, T. Jiang, Y. Hao, J. Zhang, W. Li, Y. Hao, W. He, Y. Song, Q. Feng, W. Ma, *Int. J. Pharm.* **2021**, *606*, 120937.

[93] S. Wang, X. He, Q. Wu, L. Jiang, L. Chen, Y. Yu, P. Zhang, X. Huang, J. Wang, Z. Ju, *Haematologica* **2020**, *105*, 2071.

[94] T. Stueber, M. J. Eberhardt, Y. Caspi, S. Lev, A. Binshtok, A. Leffler, *Cell Calcium* **2017**, *68*, 34.

[95] R. Zhao, S. Y. Tsang, *J. Cell. Physiol.* **2017**, *232*, 1957.

[96] J. Song, J.-B. Pan, W. Zhao, H.-Y. Chen, J.-J. Xu, *Chem. Comm.* **2020**, *56*, 6118.

[97] M. Zhou, B. Li, N. Li, M. Li, C. Xing, *ACS Appl. Bio Mater.* **2022**, *5*, 2834

[98] R. Zalk, O. B. Clarke, A. des Georges, R. A. Grassucci, S. Reiken, F. Mancia, W. A. Hendrickson, J. Frank, A. R. Marks, *Nature* **2015**, *517*, 44.

[99] D. R. Gonzalez, F. Beigi, A. V. Treuer, J. M. Hare, *P. Natl. Acad. Sci. USA* **2007**, *104*, 20612.

[100] X. Chu, X. Jiang, Y. Liu, S. Zhai, Y. Jiang, Y. Chen, J. Wu, Y. Wang, Y. Wu, X. Tao, X. He, W. Bu, *Adv. Funct. Mater.* **2021**, *31*, 2008507.

[101] S. Kakizawa, T. Yamazawa, Y. Chen, A. Ito, T. Murayama, H. Oyamada, N. Kurebayashi, O. Sato, M. Watanabe, N. Mori, K. Oguchi, T. Sakurai, H. Takeshima, N. Saito, M. Iino, *EMBO J.* **2012**, *31*, 417.

[102] H. Hao, M. Yu, Y. Yi, S. Sun, X. Huang, C. Huang, Y. Liu, W. Huang, J. Wang, J. Zhao, M. Wu, *Chem. Eng. J.* **2022**, *437*, 135371.

[103] P. Zhao, Z. Jin, Q. Chen, T. Yang, D. Chen, J. Meng, X. Lu, Z. Gu, Q. He, *Nat. Comm.* **2018**, *9*, 1.

[104] F. Gong, J. Xu, B. Liu, N. Yang, L. Cheng, P. Huang, C. Wang, Q. Chen, C. Ni, Z. Liu, *Chem* **2022**, *8*, 268.

[105] Y. Zhang, Y. Wang, E. Read, M. Fu, Y. Pei, L. Wu, R. Wang, G. Yang, *Antioxid. Redox Sign.* **2020**, *32*, 583.

[106] H. Zhao, L. Wang, K. Zeng, J. Li, W. Chen, Y. N. Liu, *ACS Nano* **2021**, *15*, 13188

[107] T. Tashima, *Bioorg. Med. Chem. Lett.* **2018**, *28*, 3015.

[108] H. He, S. Liu, D. Wu, B. Xu, *Angew. Chem. Int. Edit.* **2020**, *132*, 16587.

[109] T. Burnouf, P.-R. Jheng, Y.-H. Chen, L. Rethi, L. Rethi, L.-S. Lu, Y.-C. Ho, E.-Y. Chuang, *Mater. Design* **2022**, *215*, 110481.

[110] J. Wang, L. Hu, H. Zhang, Y. Fang, T. Wang, H. Wang, *Adv. Mater.* **2022**, *34*, 2104704.

[111] L. Hou, X. Gong, J. Yang, H. Zhang, W. Yang, X. Chen, *Adv. Mater.* **2022**, *34*, 2200389.

[112] Q. J. Han, X. T. Lan, Y. Wen, C. Z. Zhang, M. Cleary, Y. Sayyed, G. Huang, X. Tuo, L. Yi, Z. Xi, *Adv. Healthc. Mater.* **2021**, *10*, 2002143.

[113] V. T. Cong, W. Wang, R. D. Tilley, G. Sharbeen, P. A. Phillips, K. Gaus, J. J. Gooding, *Adv. Funct. Mater.* **2021**, *31*, 2007880.

[114] J. Shi, P. W. Kantoff, R. Wooster, O. C. Farokhzad, *Nat. Rev. Cancer* **2017**, *17*, 20.

[115] S. Sindhwani, A. M. Syed, J. Ngai, B. R. Kingston, L. Maiorino, J. Rothschild, P. MacMillan, Y. Zhang, N. U. Rajesh, T. Hoang, J. L. Y. Wu, S. Wilhelm, A. Zilman, S. Gadde, A. Sulaiman, B. Ouyang, Z. Lin, L. Wang, M. Egeblad, W. C. W. Chan, *Nat. Mater.* **2020**, *19*, 566.

[116] L. H. Fu, C. Qi, Y. R. Hu, J. Lin, P. Huang, *Adv. Mater.* **2019**, *31*, e1808325.

[117] C. Wang, J. Yang, C. Dong, S. Shi, *Adv. Therap.* **2020**, *3*, 2000110.

[118] J. Zagzag, M. I. Hu, S. B. Fisher, N. D. Perrier, *CA-Cancer J. Clin.* **2018**, *68*, 377.

[119] H. J. Lee, Y. H. Jung, G. E. Choi, J. S. Kim, C. W. Chae, J. R. Lim, S. Y. Kim, J. H. Yoon, J. H. Cho, S.-J. Lee, *Cell Death Differ.* **2021**, *28*, 184.

[120] W. Choi, N. Clemente, W. Sun, J. Du, W. Lü, *Nature* **2019**, *576*, 163.

[121] G. Favaro, V. Romanello, T. Varanita, M. Andrea Desbats, V. Morbidoni, C. Tezze, M. Albiero, M. Canato, G. Gherardi, D. De Stefani, *Nat. Comm.* **2019**, *10*, 1.

[122] S.-Y. Sun, X. Liu, W. Zou, P. Yue, A. I. Marcus, F. R. Khuri, *J. Biol. Chem.* **2007**, *282*, 18800.

[123] B. Dziegielewska, L. S. Gray, J. Dziegielewski, *Arch. Eur. J. Phy.* **2014**, *466*, 801.

[124] Y. Li, J. Lin, P. Wang, F. Zhu, M. Wu, Q. Luo, Y. Zhang, X. Liu, *ACS Nano* **2022**, *16*, 7380.

[125] W. Jiang, L. Yin, H. Chen, A. V. Paschall, L. Zhang, W. Fu, W. Zhang, T. Todd, K. S. Yu, S. Zhou, Z. Zhen, M. Butler, L. Yao, F. Zhang, Y. Shen, Z. Li, A. Yin, H. Yin, X. Wang, F. Y. Avci, X. Yu & J. Xie, *Adv. Mater.* **2019**, *31*, 1904058.

[126] S. Orrenius, B. Zhivotovsky, P. Nicotera, *Nat. Rev. Mol. Cell Bio.* **2003**, *4*, 552.

[127] X. Li, B. Ma, J. Li, L. Shang, H. Liu, S. Ge, *Acta Biomater.* **2020**, *101*, 554.

[128] Q. Zhang, L. Ma, X. Ji, Y. He, Y. Cui, X. Liu, C. Xuan, Z. Wang, W. Yang, M. Chai, X. Shi, *Adv. Funct. Mater.* **2022***, 32,* 2204182.

[129] D. Van hede, B. Liang, S. Anania, M. Barzegari, B. Verlée, G. Nolens, J. Pirson, L. Geris, F. Lambert, *Adv. Funct. Mater.* **2022**, *32*, 2105002.

[130] J. Fang, P. Li, X. Lu, L. Fang, X. Lü, F. Ren, *Acta Biomater.* **2019**, *88*, 503.

[131] Y.-Z. Huang, Y.-R. Ji, Z.-W. Kang, F. Li, S.-F. Ge, D.-P. Yang, J. Ruan, X.-Q. Fan, *Chem. Eng. J.* **2020**, *395*, 125098.

[132] S. Dong, Y. Chen, L. Yu, K. Lin, X. Wang, *Adv. Funct. Mater.* **2020**, *30*, 1907071.